

Aspirin potentiates celecoxib-induced growth inhibition and apoptosis in human non-small cell lung cancer by targeting GRP78 activity

Xiangyu Zhang[#], Jia Chen[#], Cheng Cheng[#], Ping Li, Fangfang Cai, Huangru Xu, Yanyan Lu, Nini Cao, Jia Liu, Jigang Wang, Zi-Chun Hua and Hongqin Zhuang

Ther Adv Med Oncol

2020, Vol. 12: 1–25

DOI: 10.1177/
1758835920947976

© The Author(s), 2020.
Article reuse guidelines:
sagepub.com/journals-
permissions

Abstract

Background: Aspirin has recently emerged as an anticancer drug, but its therapeutic effect on lung cancer has been rarely reported, and the mechanism of action is still unclear. Long-term use of celecoxib in large doses causes serious side effects, and it is necessary to explore better ways to achieve curative effects. In this study, we evaluated the synergistic anticancer effects of celecoxib and aspirin in non-small cell lung cancer (NSCLC) cells.

Methods: *In vitro*, we evaluated the combined effects of celecoxib (40 μM) and aspirin (8 mM) on cell apoptosis, cell cycle distribution, cell proliferation, cell migration and signaling pathways. Furthermore, the effect of aspirin (100 mg/kg body weight) and celecoxib (50 mg/kg body weight) on the growth of xenograft tumors was explored *in vivo*.

Results: Our data suggest that cancer sensitivity to combined therapy using low concentrations of celecoxib and aspirin was higher than that of celecoxib or aspirin alone. Further research showed that the anti-tumor effect of celecoxib combined with aspirin was mainly produced by activating caspase-9/caspase-3, arresting cell cycle and inhibiting the ERK-MAPK signaling pathway. In addition, celecoxib alone or in combination with aspirin inhibited the migration and invasion of NSCLC cells by inhibiting MMP-9 and MMP-2 activity levels. Moreover, we identified GRP78 as a target protein of aspirin in NSCLC cells. Aspirin induced an endoplasmic reticulum stress response by inhibiting GRP78 activity. Furthermore, combination therapy also exhibited a better inhibitory effect on tumor growth *in vivo*.

Conclusions: Our study provides a rationale for further detailed preclinical and potential clinical studies of the combination of celecoxib and aspirin for NSCLC therapy.

Keywords: apoptosis, aspirin, celecoxib, cell cycle arrest, GRP78, NSCLC

Received: 8 November 2019; revised manuscript accepted: 13 July 2020.

Introduction

In recent years, the number of people suffering from lung cancer worldwide has continued to increase due to various factors, such as environmental problems, smoking and second-hand smoke. Since lung cancer is not evident in the early stage and is mostly found in the advanced stage, the mortality rate of lung cancer remains high. Although the incidence of lung cancer in men is declining in some Western countries, the

incidence of lung cancer continues to rise worldwide.^{1,2} In China, nearly 400,000 people are diagnosed with lung cancer each year, and 300,000 patients die, of which approximately 250,000 had non-small cell lung cancer. Non-small cell lung cancer (NSCLC) accounts for approximately 85% of all lung cancer types,³ with few patients able to survive for long periods. Currently, the treatment methods for patients with lung cancer include surgery, radiotherapy and systemic

Correspondence to:

Hongqin Zhuang
School of Life Sciences,
Nanjing University, 163
Xianlin Blvd., Nanjing,
210023, China
hqzhuang@nju.edu.cn

Zi-Chun Hua
School of Life Sciences,
Nanjing University, 163
Xianlin Blvd., Nanjing,
210023, China
hzc1117@nju.edu.cn

Jigang Wang
Department of Biological
Science, National
University of Singapore,
Singapore, 117543,
Singapore
wangjigang@u.nus.edu

Xiangyu Zhang
Jia Chen
Cheng Cheng
Ping Li
Fangfang Cai
Huangru Xu
Yanyan Lu
Nini Cao
Jia Liu
The State Key Laboratory
of Pharmaceutical
Biotechnology, College
of Life Sciences, Nanjing
University, Nanjing, P. R.
China

[#]These authors
contributed equally to this
work.

therapy (such as chemotherapy, targeted therapy and immune checkpoint inhibitors), which have led to some therapeutic effects. However, the search for new treatment methods or the development of new treatment drugs remains a top priority for researchers worldwide.² Now, the combined use of drugs for clinical disease treatment is a considerably used therapy.

Non-steroid anti-inflammatory drugs (NSAIDs) are classified into two categories depending on the type of cyclooxygenase (COX) that is targeted. Non-selective inhibition of cyclooxygenase can inhibit both COX-1 and COX-2. Among the suppressors, the most common drug is aspirin, which has a long history of antipyretic, analgesic and anti-inflammatory activity. Recently, it was found that aspirin has a potential preventive effect on some cancers or precancerous lesions and exhibits unexpected effects on the treatment of colon cancer and breast cancer.⁴ In addition, it was found that aspirin can reduce the risk of lung cancer after long-term and low-dose administration, but the mechanism is still unclear.^{5,6} The other type of NSAID only selectively inhibits COX-2, and an example is celecoxib. It has been reported that COX-2 plays key roles in angiogenesis, tumor growth and differentiation and is overexpressed in many types of cancer, including lung cancer.⁶⁻⁹ Celecoxib is currently known to induce apoptosis, inhibit cell proliferation and cause cell cycle arrest during the treatment of lung cancer.¹⁰⁻¹² The specific mechanisms can be divided into two types: one mechanism relies on COX-2, and the other mechanism acts through a signaling pathway independent of COX-2.^{13,14} However, long-term use of celecoxib in the treatment of cancer may induce a series of negative effects, such as cardiovascular and gastrointestinal diseases.^{11,15} Therefore, celecoxib is currently being explored in combination with other anti-tumor drugs to bring hope to cancer patients.¹⁶

In the treatment of cancer, drug combination strategy has always been a popular approach because it can exhibit a synergistic effect of inhibiting tumor growth and differentiation while reducing the toxicity and the risk of each drug used alone.¹⁷⁻²⁰ To date, there have been no reports of the application of the combination of aspirin and celecoxib on NSCLC. Therefore, the purpose of this study was to explore the effects of aspirin and celecoxib on the growth and metastasis of NSCLC and to identify a potentially effective treatment strategy. The mechanisms of action

were also determined to clarify their synergistic effects and to improve the treatment of lung cancer.

Materials and methods

Cells, cell culture and reagents

NSCLC cell lines A549 and H1299, small cell lung cancer cells (H446 cells), human cervical cancer cells (HeLa cells), human lung adenocarcinoma cells (SPC-A1 cells), human liver cancer cells (BEL7402 cells), human colon cancer cells (HCT116 cells) and human breast cancer cells (MCF-7 cells) were purchased from the American Type Culture Collection (ATCC, Philadelphia, PA, USA). All cells were grown in Dulbecco's Modified Eagle Medium (DMEM; Invitrogen, Carlsbad, CA, USA) supplemented with 10% (v/v) fetal bovine serum (FBS; Invitrogen, Carlsbad, CA, USA), 100 U/mL penicillin and 100 µg/mL streptomycin (Invitrogen, Carlsbad, CA, USA). All cells were cultured in a humidified 5% CO₂ incubator at 37°C.

Aspirin (purity ≥99.0%), celecoxib (purity ≥99.0%), universal tissue fixative, dimethyl sulfoxide (DMSO), streptavidin beads, urea, Tris(2-carboxyethyl)phosphine (TCEP), phosphoric acid and Tris[[1-benzyl-1H-1,2,3-triazol-4-yl)methyl]amine (TBTA) were purchased from Sigma-Aldrich (St. Louis, USA). Cell culture flask and dish were purchased from NUNC (Denmark). Transwell chamber was purchased from Corning (New York, USA). Cell Counting Kit-8 (C0039), EdU cell proliferation assay kit (C0071S), One Step TUNEL Apoptosis Assay Kit (C1086) were purchased from Beyotime Biotechnology (Shanghai, China). BCA Protein Assay Kit (CW0014S) was purchased from CoWin Biosciences (Beijing, China). Biotin-azide was purchased from Click Chemistry Tools (Scottsdale, AZ, USA). Unless otherwise stated, all the other reagents used in biochemical methods were purchased from Sigma-Aldrich (St. Louis, USA). Aspirin probes (Asp-P1 and Asp-P2)²¹ were kindly supported by Dr. Jigang Wang from National University of Singapore (West Coast, Singapore). Lipo2000 was purchased from Life Technologies (Carlsbad, CA, USA). Opti-MEM was purchased from Gibco Life Technologies (Grand Island, NY, USA). Reverse transcription kit was purchased from TOYOBO (Kita-ku, Osaka, Japan). Interfering fragment was purchased from GenePharma (Shanghai, China).

Cell proliferation assay

The effects of celecoxib, aspirin or the combination of the two drugs on cell proliferation were assessed by the CCK8 assay. A549 and H1299 cells in the exponential growth phase were collected, and the cell density was adjusted to be 2×10^4 cells/mL. Cells were added to 96-well plates at 100 μ L per well, with six replicate wells in each experimental group and cultured overnight at 37°C. Aspirin (0, 2, 4, 5, 8, 10, and 16 mM) and/or celecoxib (0, 5, 10, 20, 40, 80, and 160 μ M) were added to the medium and cells were cultured for an additional 48 h. 100 μ L of a mixture of CCK8 and DMEM (1:100) were added to each well and cells were incubated at 37°C for an additional 1–2 h. The absorbance was measured using a microplate reader with a measurement wavelength of 450 nm and a reference wavelength of 550 nm.

The effects of celecoxib, aspirin or the combination of two drugs on cell proliferation were assessed by the EdU (5-ethynyl-2'-deoxyuridine) assay. A549 and H1299 cells in the exponential growth phase were inoculated into a six-well plate and cells were incubated for 12 h in the incubator. Then 40 μ M celecoxib, 8 mM aspirin or a combination of the two drugs was added and cells were cultured for additional 48 h. The EdU stock solution was diluted with DMEM medium to prepare a 50 μ M EdU working solution. The medium in the six-well plate was discarded and 50 μ M EdU working solution (200–500 μ L) was added to each well. Then cells were incubated for 2 h. After washing with phosphate buffered saline (PBS) for three times, cells were fixed with 4% (v/v) paraformaldehyde for 30 min at room temperature. Next, cells were permeabilized with 0.3% (v/v) Triton X-100 in PBS for 15 min at room temperature after washing with PBS solution containing 3% (m/v) bovine serum albumin (BSA). Then cells were incubated with Click Reaction Buffer for 30 min at room temperature in the dark. Hoechst 33342 was added to each well and incubated for 10 min in the dark at room temperature. Finally, cells were photographed by fluorescence microscope (Zeiss, Jena, Germany).

Flow cytometry

To quantify the percentage of cells undergoing apoptosis, we used the Annexin V-FITC kit as described by the manufacturer (BD Biosciences, CA, USA). Briefly, A549 and H1299 cells were incubated for 48 h with celecoxib (40 μ M) and aspirin (8 mM) alone or the combination of both

drugs. Next, treated cells were collected and trypsinized for 3–5 min. The cells were collected and centrifuged for 5–10 min using a refrigerated centrifuge (4°C, 3000 rpm), and the supernatant was carefully discarded. Then cells were softly washed with cold PBS. The cell pellets were resuspended in Hepes buffer and incubated with Annexin V-FITC (1 mg/mL) on ice for 20 min. Propidium iodide (20 μ g/mL) was added before flow cytometry analysis (BD Biosciences, CA, USA). Quantification of apoptotic cells was analyzed by CellQuest software (BD Biosciences, CA, USA).

TUNEL assay

The TdT-mediated dUTP nick end labeling (TUNEL) assay was used to evaluate the apoptosis caused by celecoxib, aspirin or the combination of the two drugs in A549 cells. A549 cells were treated with 40 μ M celecoxib, 8 mM aspirin or the combination of the two drugs for 48 h. Cells were washed twice with PBS and then fixed in 4% (v/v) paraformaldehyde and permeabilized with 0.2% (v/v) Triton X-100 in PBS for 5 min. TUNEL assay was performed with the One Step TUNEL Apoptosis Assay Kit. In brief, TUNEL detection solution was added to each sample and incubated at 37°C for 60 min. At this time, the genomic DNA of apoptotic cells was broken, and the exposed 3'-OH was catalyzed by terminal deoxynucleotidyl transferase (TdT) to add dUTP labeled by FITC. After washing with PBS, the cells were re-stained with propidium iodide (PI). The fluorescent photos of the cells were captured by a fluorescence microscope (Zeiss, Jena, Germany).

Cell cycle analysis

A549 cells were treated with 40 μ M celecoxib, 8 mM aspirin or the combination of the two drugs for 48 h. The cells were digested with trypsin and centrifuged for 4 min (4°C, 800 rpm) in a refrigerated centrifuge, and the pellets were washed twice with PBS. Cells were fixed overnight at 4°C using 70% pre-cooled ethanol and then centrifuged for 10–15 min (4°C, 3000 rpm). Fixed cells were washed and stained with PI (2 mg/mL) in PBS with RNase A (0.1 mg/mL) for 30 min at room temperature in the dark. The distribution of cells with differing DNA content was analyzed on a FACSCalibur flow cytometer with CellQuest software (BD Biosciences, CA, USA) at an excitation wavelength of 530 nm. Fluorescence emission was measured using a 620 nm band pass filter.

Measurement of reactive oxygen species

NSCLC cells were treated with 40 μ M celecoxib, 8 mM aspirin or the combination of the two drugs for 48 h. After digesting, cells were centrifuged for 5 min (4°C, 2000 rpm) using a refrigerated centrifuge, and then washed with PBS. Next, cells were resuspended in serum-free DMEM medium containing 10 μ M 2,7-Dichlorodi-hydrofluorescein diacetate (DCFH-DA) (Beyotime Biotechnology, Shanghai, China) and incubated at 37°C for 30 min in the dark. After centrifugation, cells were collected and washed with PBS three times, and then analyzed by a FACSCalibur flow cytometer with CellQuest software (BD Biosciences, CA, USA) with a 400 μ L single cell suspension. The level of intracellular reactive oxygen species (ROS) was determined based on the fluorescence intensity of the FL1 channel.

Mitochondrial membrane potential

A549 cells were treated with 40 μ M celecoxib, 8 mM aspirin or the combination of the two drugs for 48 h. The residual medium was washed off with PBS, and then 5,5',6,6'-Tetrachloro-1,1',3,3'-tetraethyl-imidacarbocyanine iodide (JC-1) staining solution was added in the dark and discarded after incubation for 20–30 min at 37°C. Then, after washing with PBS for three times, 1 \times Hoechst 33342 reaction solution was added in the dark for 5 min to observe the fluorescence of the cells under a fluorescence microscope.

Cytoskeleton staining

NSCLC cells were seeded on sterilized coverslips for growth. When the cells grew to 40–50% confluence, 40 μ M celecoxib, 8 mM aspirin or a combination of these two drugs was added, and cells were further cultured for 48 h. After washing with PBS, pre-cooled 4% paraformaldehyde was added and cells were fixed overnight at 4°C. The remaining fixative was washed off with pre-cooled PBS, and then placed at 0.5% Triton X-100 for 2 h at room temperature. After washing with PBS, the anti-F-Actin/FITC (fluorescein isothiocyanate) dilution (diluted with PBS containing 1% BSA, 1:40) was used for staining for 40 min in the dark, and the nuclei were stained for 2 min using a DAPI (2-(4-Amidinophenyl)-6-indolecarbamide dihydrochloride) staining solution (Beyotime Biotechnology, Shanghai, China). Finally, 20 μ L of the antifade mounting medium was slowly added dropwise to the coverslip and cells were observed under a fluorescence microscope.

Transwell assay

The effects of celecoxib, aspirin or their combination on tumor cell migration were assessed by the Transwell assay using Transwell inserts (8.0 mm pore size, Millipore, Billerica, MA, USA). First, H1299 cells were cultured in serum-free medium for 12 h. Then the cells were harvested and resuspended in serum-free DMEM containing 40 μ M celecoxib, 8 mM aspirin or the combination of the two drugs. A total of 200 μ L of cell suspension with a density of 5×10^5 cells/mL were pipetted into the upper chamber, and the lower chamber was filled with 600 μ L of 10% FBS supplemented medium. After incubation at 37°C for 10 h or 16 h, cells on the upper surface of the membrane were removed. The migrant cells attached to the lower surface were fixed in 4% paraformaldehyde at room temperature for 30 min, and stained for 30 min with a solution containing 1% crystal violet and 2% ethanol in 100 mM borate buffer (pH 9.0). The number of cells migrating to the lower surface of the membrane was photographed in five fields under a microscope at a magnification of 100 \times . The chamber was then purged with 33% HOAc (acetic acid; 100 μ L). After the crystal violet was completely dissolved and the cells were evenly distributed in the HOAc solution, the assay was performed using a microplate reader (TECNA, Switzerland) at 570 nm and quantitative analysis was performed using GraphPad Prism v8.0 software.

Wound-healing assay

Cells were plated in 12-well culture plates to form a cell monolayer (near 90% confluence). After serum starvation for 12 h, a wound was made by scraping off the cells with a sterile P-200 micropipette. The wells were washed three times with PBS to remove non-adherent cells and then incubated with celecoxib (40 μ M), aspirin (8 mM) or a combination of these two drugs in medium containing 10% FBS for 48 h. The progress of wound closure was monitored with microphotographs of 10 \times magnification taken with a light microscope (Carl Zeiss Axioplan 2) at the beginning and the end of the experiments.

Western blotting analysis

Whole cell lysate was prepared with RIPA buffer (Santa Cruz Biotechnology) containing protease inhibitors, phenylmethylsulfonyl fluoride (PMSF) and sodium orthovanadate. Supernatants were collected and protein concentrations were determined by the Bio-Rad protein assay method

(Bio-Rad, Hercules, CA, USA). Western blotting analysis used standard protocols. Proteins were separated by SDS-PAGE and transferred onto nitrocellulose membranes that were blocked with 5% non-fat milk in Tris-buffered saline (TBS) containing 0.1% Tween-20, and incubated with primary antibodies: cleaved caspase-3, cleaved caspase-7, cleaved caspase-8, cleaved caspase-9, caspase-12, cleaved PARP, Bcl-2, Bcl-xl, Bax, extracellular signal-regulated kinase (ERK), pERK, MEK, pMEK, Ras, Raf, pRaf, GRP78 (Cell Signaling Technology, Beverly, MA, USA), β -actin, α -tubulin (ABGENT, San Diego, USA). Secondary antibodies were coupled to horseradish peroxidase, and were goat anti-rabbit or goat anti-mouse. Bound antibodies were then visualized with electrochemiluminescence (ECL) plus western blotting detection reagents (GE Healthcare). Signal intensity was quantified by densitometry using the software Image J (NIH, Bethesda, MD, USA). All experiments were done in triplicate and performed at least three times independently.

Enrichment of target proteins in cells

When A549 cells grew to 80–90% confluence, the culture condition was changed to culture medium (1% DMSO) containing 20 μ M aspirin probe (Asp-P1 or Asp-P2)²¹ (experimental group) or medium without probe (negative control). After that, the cells continued to be cultured at 37°C for 12h. Then cells were lysed using 150mM NaCl and 1% Triton X-100, and the insoluble debris was removed by centrifugation at 10,000rpm for 45min. After detecting concentration, the protein solution was used for “click chemistry” (copper-catalyzed azide-alkyne cycloaddition; CuAAC) reaction. Briefly, 4mg protein was incubated with 10 μ M biotin-azide, 1mM TCEP, 100 μ M TBTA and 1mM copper sulfate for 4h at room temperature, and then precipitated and dried with ice acetone. After the protein precipitations were re-dissolved with PBS (containing 1.2% SDS), streptavidin beads were added and incubated for 4h at room temperature. Then streptavidin beads were washed sequentially with PBS containing 1% SDS, PBS containing 0.1% SDS, 6 M urea solution, PBS and double distilled water. After dissolving the streptavidin beads with 1 \times SDS loading buffer, the protein samples were separated by SDS-PAGE and immunized with the specific antibody for GRP78. All experiments were done in triplicate and performed at least three times independently.

Expression and purification of protein

Homologous recombination was used to construct the expression plasmid pET28a-GRP78-EGFP. Briefly, the gene sequence of GRP78 was synthesized in pET28a at the NdeI and XhoI restriction sites to generate pET28a-GRP78. The EGFP gene was PCR amplified using primers GRP78-EGFP-F and GRP78-EGFP-R from pUC18-EGFP kept in our lab (Supplemental Material Table 1online). The amplified EGFP fragment was ligated into linearized vector pET28a-GRP78 amplified with primers pET28a-GRP78-F and pET28a-GRP78-R generating pET28a-GRP78-EGFP (Supplemental Figure 1). More details about the plasmid pET28a-GRP78-EGFP are provided in the Supplemental Methods. The bacterial solution containing the recombinant plasmid pET28a-GRP78-EGFP was cultured in liquid LB medium containing 50 μ g/mL kanamycin at 37°C. When the OD₆₀₀ value reached 0.6–0.7, the expression of the target protein was induced by adding 1mmol/L of isopropyl- β -D-thiogalactoside at 16°C for an additional 16–20h. The cells were pelleted by centrifugation for 15min (4°C, 6000rpm) using a refrigerated centrifuge. After washing with pre-cooled Hepes-NaCl buffer, cells were centrifuged again for 15min under the same conditions. The cells were then placed in a Ni Binding Buffer and subjected to high pressure sonication under ice bath conditions until the bacterial solution was clear. The collected supernatant was filtered through a filter (pore size 0.22 μ m). Ni was added to the column for filling, and the target protein GRP78 protein was collected by affinity chromatography.^{22,23} Next, ammonium sulfate solid (mass fraction 20–30%) was added to the collected liquid, and the mixture was stirred overnight at 4°C to sufficiently precipitate the protein of interest. The precipitated protein was separated by SDS-PAGE. The purity of the protein of interest was analyzed and the concentration was determined using the BCA assay.

Microscale thermophoresis (MST)

The aspirin solution (100mM or 500mM) was diluted by gradient dilution. The dilution ratio was 1:1, and a total of 14 concentrations were diluted. A total of 10 μ L of 200nM GRP78 protein was added to each concentration of aspirin solution. After incubating for 5min at room temperature in the dark, the binding ability was measured using a microscale thermophoresis (Monolith NT.115, NanoTemper Technologies, Munich, Germany) according to the manufacturer’s instructions.

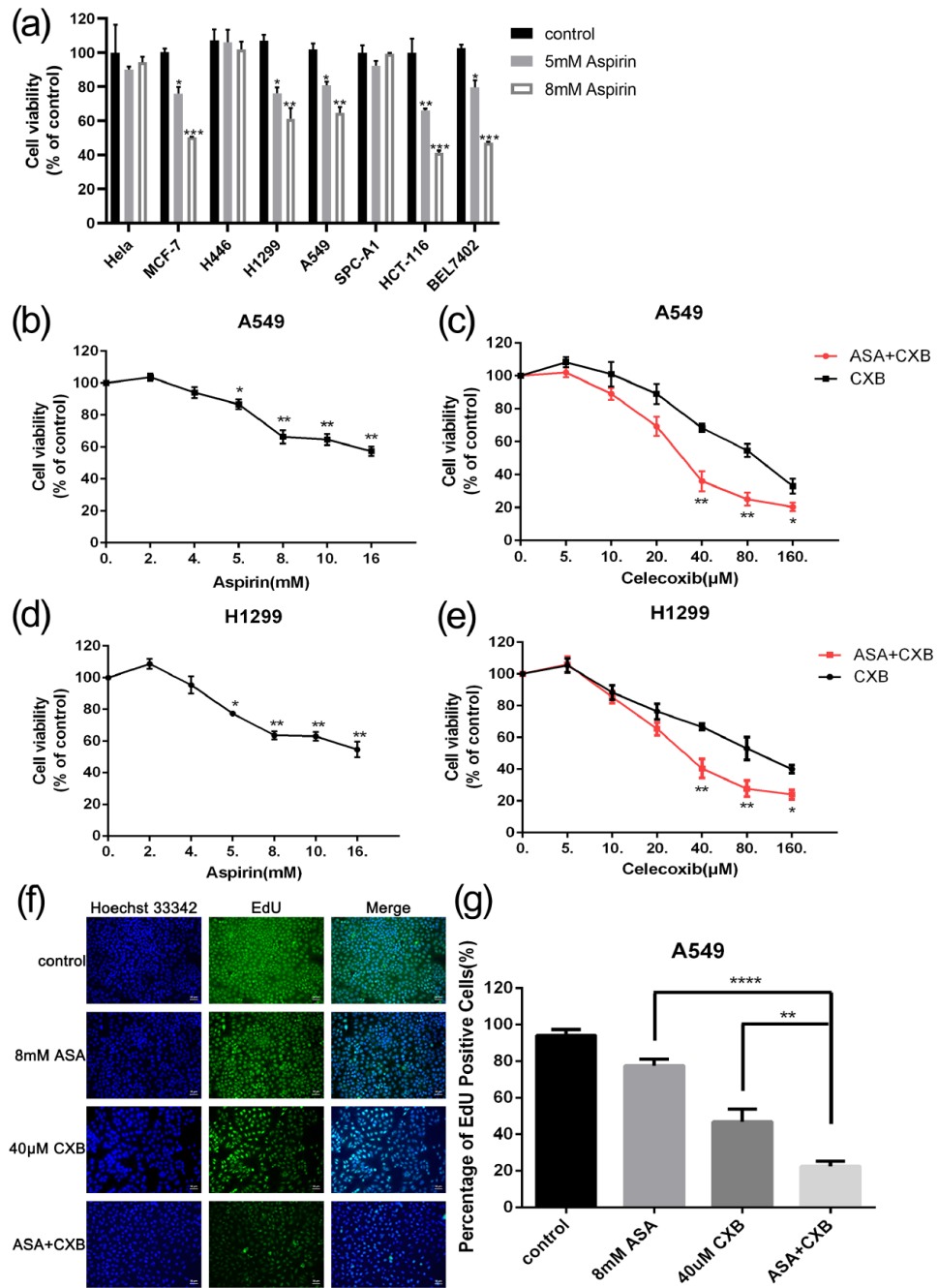


Figure 1. Effect of celecoxib and aspirin on the growth of tumor cells. (a) A549, H1299, HeLa, SPC-A1, H446, BEL7402, HCT116 and MCF-7 cells were treated with 5 mM or 8 mM aspirin for 48 h, and the cell viability was assessed by CCK8 assay. (b) and (d) A549 and H1299 cells were treated with different concentrations of aspirin (0, 2, 4, 5, 8, 10, and 16 mM) for 48 h, and the cell viability was assessed by CCK8 assay. (c) and (e) A549 and H1299 cells were treated with different concentrations of celecoxib (0, 5, 10, 20, 40, 80, and 160 µM) alone or in combination with 8 mM aspirin for 48 h, and the cell viability was assessed by CCK8 assay. (f) and (g) A549 and H1299 cells were exposed to celecoxib (40 µM) and/or aspirin (8 mM) and incubated with the EdU-DMEM mixture for 2 h. Four percent paraformaldehyde was used to fix cells and 0.5% Triton X-100 was used for perforation of cell membranes. The staining solution was added according to the instructions of the EdU kit, and the fluorescence of the cells was observed. Data are represented as mean ± SD. *****p* < 0.0001

ASA, aspirin; CXB, celecoxib; DMEM, Dulbecco's Modified Eagle Medium; EdU, 5-ethynyl-2'-deoxyuridine.

Transfection of interference fragments

A549 cells were cultured until the density reached about 40% and the GRP78 interference fragment was transfected. The interference fragment (siGRP78) sequence was 5'-AAGAUCACAAUCACCAAUGACTT-3'; the control sequence was 5'-AAAUCAUAGCGUAUGGUGCUGTT-3'. The siGRP78 fragment and lipo2000 were dissolved using Opti-MEM respectively, and then they were mixed and allowed to incubate at room temperature for 20 min. Then, the mixture was added to A549 cells and the medium was replaced with DMEM containing 10% FBS after 4–6 h. Cells were harvested 48 h later and the transfection effect was detected by western blotting analysis.

Animals

Female healthy athymic nude mice (5–6 weeks of age) were obtained from Changzhou Cavens Laboratory Animal Co., Ltd. (Changzhou, China) and housed under germfree conditions. All animals received humane care according to Chinese legal requirements. The experiments were approved by Nanjing University Animal Care and Use Committee (#IACUC_1911016), and we strictly followed these rules during our experiments.

In vivo xenograft tumor model of human NSCLC

A549 cells (1×10^6 cells in 100 μ L) were injected subcutaneously under the right axilla of the mice. Tumor volume was monitored by measuring the two maximum perpendicular tumor diameters with vernier caliper every other day. All tumor-bearing mice were randomly divided into four groups: the control group, the aspirin group, the celecoxib group and the combination group. When the tumor reached about 100–150 mm³ on the eighth day, the treatment was initiated. Aspirin (100 mg/kg body weight) was dissolved in PBS and used as daily drinking water for mice in the aspirin group or the combination group. The mice in the celecoxib group or the combination group were injected intraperitoneally (i.p.) with celecoxib (50 mg/kg body weight) dissolved in 100% DMSO every other day. Control mice were given sterile water daily and received i.p. injection of DMSO for the same period of time as the drug treatment groups. The drug treatment cycle was 28 days. Mice were weighed every two days and the maximum vertical length of all measurable tumors was measured using a vernier caliper every other day. Anti-tumor activity of treatments was evaluated by tumor growth inhibition. The formula, tumor

volume = length \times width² \times 0.52 was used to mimic the tumor volume. At the end of the study, the tumors were collected and weighed. In a parallel animal assay (totally four groups, and six mice per group), the tumor establishment and drug treatment are the same as described previously. On the 28th day, mice were euthanized. Tumors were collected, fixed with 4% paraformaldehyde, embedded in paraffin and sectioned for hematoxylin-eosin (HE) staining according to standard histological procedures.²⁴ Apoptotic cells in tumor sections (two sections per mouse, four mice in total) were visualized by the TUNEL technique and further verified by immunohistochemistry using anti-cleaved caspase-3.

Calculation of tumor doubling time and tumor inhibition rate

For calculating tumor doubling time (TDT), the equation of Schwartz²⁵ was used:

$$\text{TDT} = \frac{t}{10 \times \log \left(\frac{D_t}{D_0} \right)} \quad (1)$$

Where t is the total number of treatment days, D_0 is the diameter at the start of treatment, D_t is the diameter after time t , and the diameter is expressed as $1/2 \times (\text{length} + \text{width})$.

For calculating tumor growth inhibition value (TGI), the formula (2) was used:

$$\text{TGI} = \left(1 - \frac{W_t}{\frac{W_{t_0}}{n}} \right) \times 100\% \quad (2)$$

Where t is the total number of treatment days, W_t is the tumor weight of the treatment group after time t , W_{t_0} is the tumor weight of the control group after time t , and n is the number of mice in the control group.

All data statistics were performed using GraphPad Prism v8.0.

Statistical analysis

Statistical analysis was carried out using the SPSS software (version 11.0; SPSS, Chicago, IL, USA). Data were expressed as the mean \pm standard

deviation (SD). For paired data, statistical analyses were performed using two-tailed Student's *t*-tests. For multiple comparisons, statistical analyses were performed using one-way analysis of variance with a Tukey post-test. For all analyses, $p < 0.05$ was considered statistically significant.

Results

Combined effect of celecoxib and aspirin on the growth of NSCLC cells

Aspirin at doses of 5 mM and 8 mM inhibited the proliferation of cells from various lineages, such as A549, H1299, HeLa, SPC-A1, H446, BEL7402, HCT116 and MCF-7 cells, as assessed by CCK-8 assay after 48 h of drug exposure. As shown in Figure 1(a), the viability of the A549, H1299, HCT116, BEL7402 and MCF-7 cells treated with 5 mM aspirin was approximately 70–80% that of the control group. Following treatment with 8 mM aspirin, the viability of the A549 and H1299 cells was approximately 60% that of the control group ($p < 0.001$), and the viability of the HCT116, BEL7402 and MCF-7 cells was lower than 45% ($p < 0.001$), while for the HeLa, SPC-A1 and H446 cells, no significant inhibition of proliferation was observed. These results indicate that aspirin can inhibit the proliferation of various cancer cells, such as A549 and H1299 cells, and 8 mM aspirin treatments inhibited cell proliferation more effectively than did 5 mM aspirin treatments. Since the anti-tumor effects of aspirin reported in the literature are mostly related in colorectal cancer and breast cancer with few reports on lung cancer,²⁶ and because A549 and H1299 cells are relatively sensitive to aspirin, A549 and H1299 cells were selected as the main research objects for the experiments.

Before testing the combined effects of celecoxib and aspirin, we first treated A549 and H1299 cells with different concentrations of aspirin (0, 2, 4, 5, 8, 10, and 16 mM) for 48 h, and then measured their viability by CCK-8 assay. As shown in Figure 1(b) and (d), the cell viability of the 5 mM aspirin group was approximately 80%, and the cell viability of the 8 mM aspirin group was approximately 60% for both the A549 and H1299 cells, which was significantly different from that of the control group ($p < 0.01$). Subsequently, the A549 and H1299 cells were treated with different concentrations of celecoxib (0, 5, 10, 20, 40, 80, and 160 μ M) alone or in combination with 8 mM aspirin for 48 h. A CCK-8 assay was used to

measure cell proliferation, and we found that celecoxib alone could inhibit NSCLC cell proliferation in a dose-dependent manner, while celecoxib combined with aspirin showed greater inhibition of proliferation [Figure 1(c) and (e)]. At a concentration of 20 μ M or lower, celecoxib induced no significant difference in cell viability between the combination group and the celecoxib monotherapy group. At a concentration of 40 μ M celecoxib, the combination of celecoxib and aspirin inhibited cell proliferation more significantly than did celecoxib alone ($p < 0.01$). Thus, we chose 8 mM aspirin and 40 μ M celecoxib as the concentrations for the combination therapy in our subsequent study.

To further detect the inhibition of A549 cell proliferation by celecoxib combined with aspirin, an EdU assay was performed. EdU, similar to thymine T, can be incorporated during cell replication. Through the subsequent click reaction, EdU was labeled by Alexa Fluor 488 to display the double helix structure of DNA, and the proliferation phenomenon was directly observed under a fluorescence microscope. The results are shown in Figure 1(f) and (g). In the aspirin-treated or celecoxib-treated group, the proportion of EdU-positive cells decreased, while the proportion of EdU-positive cells in the combined group decreased most significantly, indicating their synergistic inhibitory effect on the proliferation of cancer cells at relatively low concentrations. Together, these results showed that celecoxib at a subtoxic concentration had an enhanced effect on the aspirin-inhibited proliferation of tumor cells.

Combined effect of celecoxib and aspirin on tumor cell apoptosis

To determine whether tumor cellular viability was reduced with celecoxib and aspirin *via* apoptosis, two NSCLC cell lines (A549 and H1299) were exposed to celecoxib (40 μ M), aspirin (8 mM) or a combination of both, and the apoptosis ratio was measured. As shown in Figure 2(a), no significant apoptosis was observed for the NSCLC cells treated with aspirin alone, while a single treatment of celecoxib induced a 13–20% apoptosis ratio. However, when the A549 and H1299 cells were treated with aspirin and celecoxib in combination, the number of cells undergoing apoptosis markedly increased (35–43%). A TUNEL assay was also performed to determine the effect of the two drugs on NSCLC

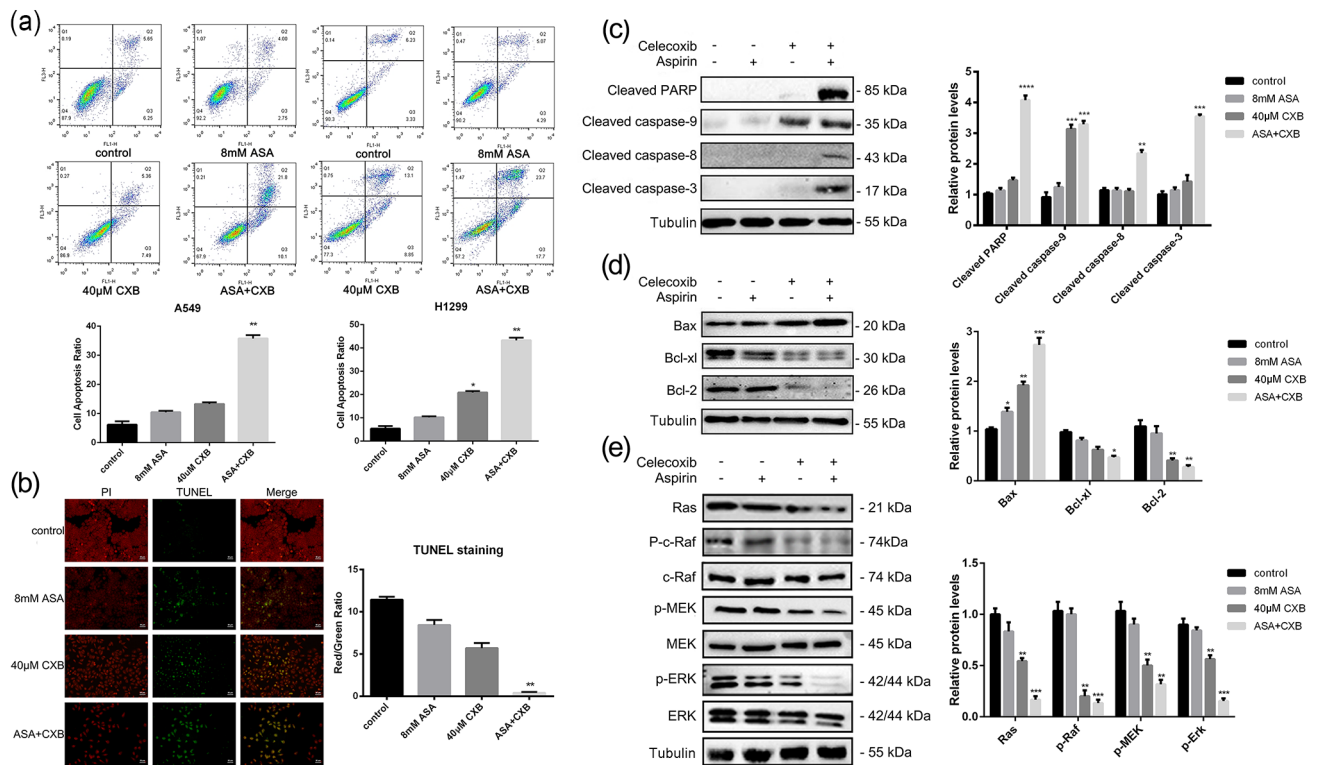


Figure 2. Aspirin enhances celecoxib-induced cell apoptosis. (a) A549 and H1299 cells were exposed to celecoxib (40 μM) and/or aspirin (8 mM); 48 h later, all cells were harvested for flow cytometry analysis. Annexin V/PI-stained cells were analyzed and the percentage of apoptotic cells was determined. The experiments were carried out independently in triplicate; representative data are shown. Annexin V/PI double staining profile of A549 cells is also included. (b) A549 and H1299 cells were exposed to celecoxib (40 μM) and/or aspirin (8 mM) for 48 h. TUNEL assays were performed according to the manufacturer's instructions. The rate of apoptosis was expressed as the percentage of total cells counted. TUNEL staining profile of A549 cells is also shown. (c) Activation of caspase-3, -8 and -9 in A549 cells treated with celecoxib and aspirin alone or in combination for 48 h was detected by western blotting analysis. (d) Expression levels of the Bcl-2 family proteins, Bcl-2, Bcl-xl and Bax in A549 cells under different treatment conditions. (e) Expression levels of Ras, p-c-Raf, c-Raf, p-MEK, MEK, p-ERK, and ERK in A549 cells under different treatment conditions. All gels run under the same experimental conditions and the representative images of three different experiments are cropped and shown. Band intensity was quantified by Image J software. Data are represented as mean ± SD.

* $p < 0.05$

** $p < 0.01$

*** $p < 0.001$

**** $p < 0.0001$

ASA, aspirin; CXB, celecoxib; PARP, poly(ADP-ribose) polymerase; PI, propidium iodide; TUNEL, TdT-mediated dUTP nick end labeling.

cell apoptosis. As shown in Figure 2(b), A549 cells treated with celecoxib or aspirin alone for 48 h showed a slightly increased green fluorescence ratio, indicating a low apoptosis rate. The ratio of green fluorescence in the combination group was significantly increased, indicating a large increase in the number of cells undergoing apoptosis. Therefore, by TUNEL assay, we also found that aspirin and celecoxib in combination induced significant apoptosis compared with the single therapy with either drug alone, a finding consistent with the results obtained from the flow cytometry analysis.

Celecoxib and aspirin induce apoptosis in a caspase-dependent manner and via the inhibition of the ERK-MAPK signaling pathway

To explore the mechanisms underlying celecoxib- and aspirin-triggered apoptosis in A549 cells, the expression of pro-apoptotic proteins and caspase activation was measured by western blotting. Caspases are the main enzymes involved in the induction of apoptosis. As shown in Figure 2(c), celecoxib and aspirin alone did not cause apparent caspase-8 or caspase-3 cleavage, while celecoxib alone caused caspase-9 cleavage. In contrast, celecoxib combined with aspirin caused more

pronounced proteolytic cleavage of caspase-8, -9 and -3. In addition, the combination of the two drugs resulted in the cleavage of poly(ADP-ribose) polymerase (PARP), whereas neither celecoxib nor aspirin alone induced PARP cleavage. These results suggest that the caspase-mediated apoptotic pathway may be one of the main mechanisms by which apoptosis is induced in A549 cells treated with a combination of aspirin and celecoxib.

Next, we investigated the combined effects of celecoxib and aspirin on anti-apoptotic proteins (Bcl-xl or Bcl-2) and pro-apoptotic protein (Bax) in A549 cells. As shown in Figure 2(d), the expression levels of Bcl-xl, Bcl-2 and Bax in the 8 mM aspirin-treated group were not significantly different as compared with the control group, while the expression of Bcl-xl and Bcl-2 was down-regulated and the level of Bax was slightly up-regulated in the 40 μ M celecoxib-treated group. However, the combination of aspirin and celecoxib noticeably elevated the level of Bax and induced a prominent decrease in Bcl-xl and Bcl-2 levels. These results indicate that celecoxib combined with aspirin induced the apoptosis of A549 cells *via* the caspase-mediated mitochondrial pathway.

To further explore the mechanism by which aspirin and celecoxib inhibit cell proliferation and induce cell apoptosis, the phosphorylation and total protein levels of ERK protein and its upstream MEK, Raf and Ras proteins in A549 cells were also measured by western blotting analysis following treatment with aspirin and/or celecoxib. The results are shown in Figure 2(e). We found that the phosphorylation level of the ERK protein in the combination group was significantly down-regulated; however, no apparent changes were observed in the aspirin or celecoxib single therapy groups. In addition, the combination of aspirin and celecoxib induced a significant increase in the phosphorylation levels of MEK and Raf and the protein level of Ras. In contrast, treatment with aspirin alone failed to activate the MEK-ERK signaling pathway, while celecoxib treatment alone led to only slightly decreased levels of ERK, MEK and Raf phosphorylation. Overall, these findings suggested that the combination of aspirin and celecoxib inhibited the phosphorylation of ERK protein and its upstream proteins, implying that the ERK signaling pathway is probably among the main mechanisms accounting for aspirin and celecoxib-induced apoptosis.

Combined effect of celecoxib and aspirin on ROS and mitochondrial membrane potential levels

Previous reports suggested that celecoxib can kill cancer cells by inducing ROS generation.²⁷ Next, we evaluated ROS generation following celecoxib and/or aspirin treatment of NSCLC cells by flow cytometry analysis. After treatment with celecoxib or aspirin alone for 48 h, A549 and H1299 cells had slightly increased ROS levels; however, the combination of these two drugs caused significant accumulation of ROS [Figure 3(a)]. In addition, we also found that the loss of mitochondrial membrane potential was more pronounced in the A549 cells treated with celecoxib and aspirin in combination than it was with either single-drug treatment [Figure 3(b)]. Taking these results together, we thus concluded that celecoxib combined with aspirin caused an increase in ROS levels and a decrease in mitochondrial membrane potential in the A549 and H1299 cells, suggesting that the combination of these two drugs causes oxidative stress and mitochondrial damage in NSCLC cells.

Combined effect of celecoxib and aspirin on NSCLC cell migration

To investigate the effect of celecoxib and aspirin on tumor cell migration, wound healing and Transwell assays were conducted. A Transwell motility chamber assay was used to determine the number of cells that cross the migration chamber membrane after treatment with celecoxib and aspirin alone or in combination for 48 h. As shown in Figure 4(a), when 40 μ M celecoxib or 8 mM aspirin was used alone, the number of H1299 cells passing through the chamber membrane was slightly decreased, but the differences compared with the control group were not significant. However, when the two drugs were used in combination, the number of H1299 cells passing through the chamber membrane was found to be significantly reduced ($p < 0.05$). Furthermore, the effect of aspirin and celecoxib on cell migration was also verified by wound-healing experiments. Celecoxib and aspirin were used to treat A549 and H1299 cells alone or in combination. After the cells were cultured for 24 h, a scratch test was performed to detect the cell growth and migration into the scratch. As shown in the lower panel of Figure 4(b), in A549 cells, compared with the control group, the scratch-healing rate of the aspirin treatment group decreased slightly but not significantly. The celecoxib single-treatment group

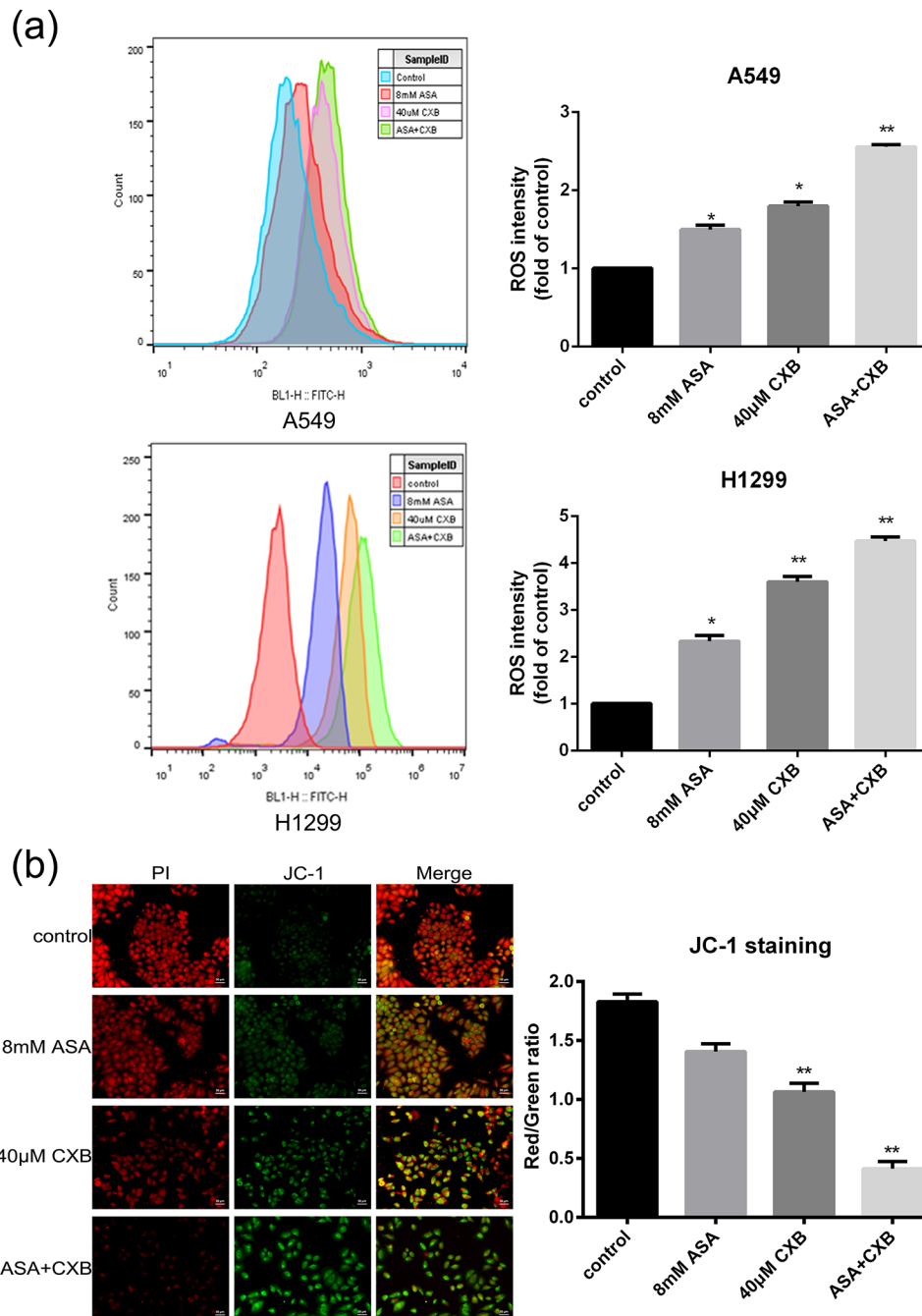


Figure 3. The effect of celecoxib and aspirin on ROS and MMP levels in NSCLC cells. (a) A549 and H1299 cells were exposed to celecoxib (40 µM) and/or aspirin (8 mM); 48 h later, 10 µM DCFH-DA was added and incubated for 30 min, and then all cells were harvested for flow cytometry analysis. (b) A549 cells were exposed to celecoxib (40 µM) and/or aspirin (8 mM); 48 h later, JC-1 was added and incubated for 20–30 min in the dark. Then cells were observed and photographed with a fluorescence microscope. Data are represented as mean ± SD.

* $p < 0.05$

** $p < 0.01$

ASA, aspirin; CXB, celecoxib; MMP, matrix metalloproteinase; NSCLC, non-small cell lung cancer; DCFH-DA, 2,7-Dichlorodihydrofluorescein diacetate; PI, propidium iodide; JC-1, 5,5',6,6'-Tetrachloro-1,1',3,3'-tetraethyl-imidacarbocyanine iodide; ROS, reactive oxygen species.

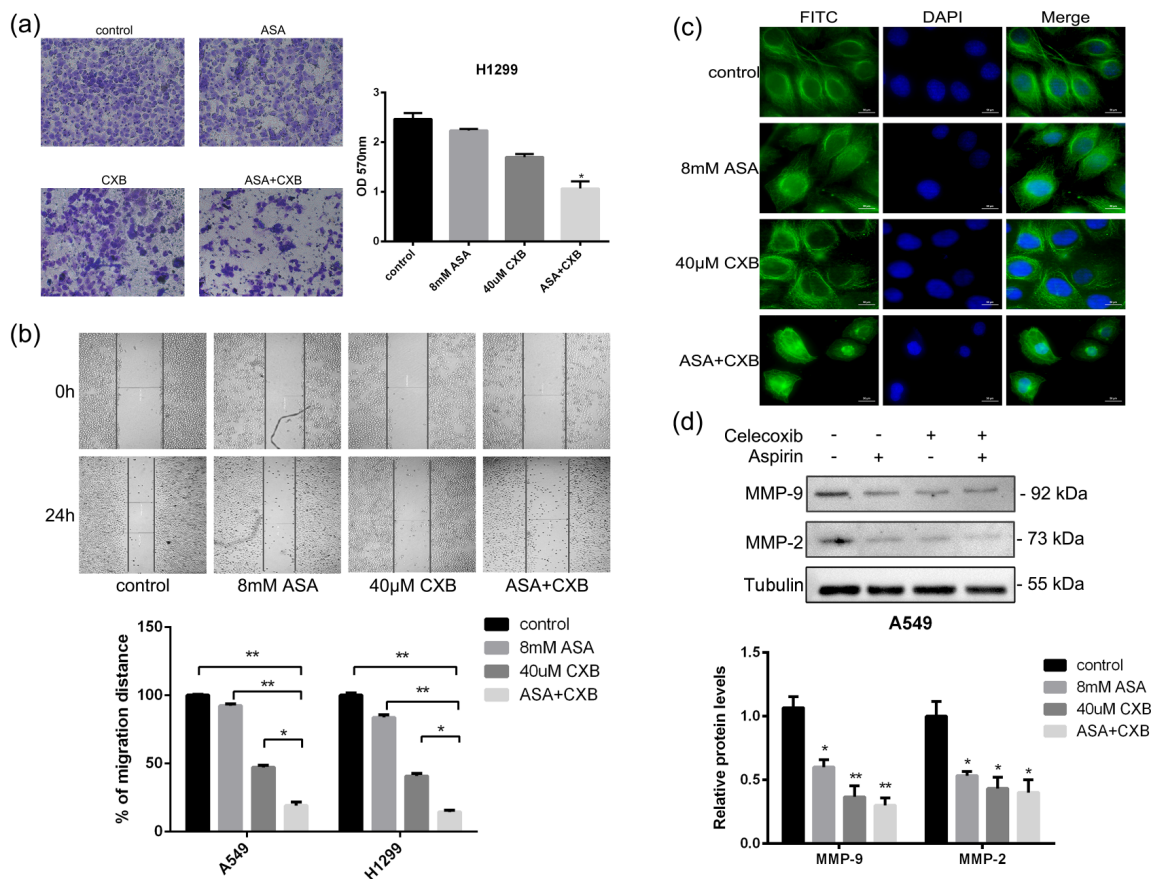


Figure 4. Effect of celecoxib and aspirin on non-small cell lung cancer cell migration. (a) Transwell assay. H1299 cells were treated with celecoxib (40 μ M) and/or aspirin (8 mM). After 16 h pretreatment and 12 h incubation in the upper chamber, the cells migrating to the lower membrane were stained and counted in five fields. (b) Wound healing assays. A549 and H1299 cells were treated with celecoxib (40 μ M) and/or aspirin (8 mM). Photographs were taken immediately and after 48 h of creating the scratch. Images shown are representative of three independent experiments. Relative scratch covered area was quantified by Image J from four areas. (c) A549 cells were exposed to celecoxib (40 μ M) and/or aspirin (8 mM); 48 h later, immunofluorescence was carried out to display F-actin (Anti-F-Actin/FITC, green), and nuclei (DAPI, blue) in A549 cells. (d) Effects of celecoxib and aspirin on MMP-2 and MMP-9 protein expression. A549 cells were treated with celecoxib (40 μ M) and/or aspirin (8 mM); 48 h later, cells were harvested for western blotting analysis using indicated antibodies. The level of tubulin served as the loading control. Band intensities were calculated using software Image J. The results shown are representative of three different experiments. Data are represented as mean \pm SD.

* $p < 0.05$

** $p < 0.01$

ASA, aspirin; CXB, celecoxib; FITC, fluorescein isothiocyanate; DAPI, 2-[4-Amidinophenyl]-6-indolecarbamidine dihydrochloride.

showed a significantly reduced scratch healing rate, and the healing rate decreased the most significantly for the combined group. Similar results were also observed in H1299 cells. Moreover, F-actin staining was performed to observe the morphology of the cytoskeleton. As shown in Figure 4(c), compared with the control group, the microfilament structure in the cytoskeleton of the A549 cells was shorter after treatment with aspirin alone, but the cell arrangement was still ordered;

however, the microfilament structure of the cytoskeleton was changed in the celecoxib treatment group. The extent of the shortening was more obvious; the cell morphology was enlarged and not fusiform. The microfilament structure of the cytoskeleton in the combination group was shortened the most significantly, and the sorting order changed from being bunched together to being disordered. Taken together, these data suggest that the combination of aspirin and celecoxib

inhibited the migration of NSCLC cells by modulating the cytoskeletal machinery that is required for cell motility.

Many proteins have been found to be closely related to the mechanism of lung cancer metastasis, and matrix metalloproteinases (MMPs) are hotspots in research. MMP-2 and MMP-9 are members of the MMP family and play pivotal roles in cell migration. A number of research papers describe the role of MMP-2 and MMP-9 in different malignant progression cases.²⁸ Therefore, we next used western blot analysis to detect changes in the expression levels of MMP-2 and MMP-9 proteins after treatment with aspirin or celecoxib alone or both drugs in combination. As shown in Figure 4(d), the results show that aspirin and celecoxib alone led to a reduction in the levels of MMP-2 and MMP-9 proteins compared with the control group ($p < 0.05$). When the two drugs were combined, the down-regulation of the expression of MMP-2 and MMP-9 proteins in A549 cells was the most significant. Collectively, these findings indicated that the effects of aspirin and celecoxib on the protein expression of MMP-2 and MMP-9 might account for their inhibitory effect on NSCLC cell migration.

Celecoxib and aspirin in combination initiate cell cycle arrest at the G0/G1 phase in NSCLC cells

Celecoxib has been reported to have the ability to inhibit cell proliferation to execute its anti-tumor effect.²⁹ Therefore, we examined the effect of aspirin, celecoxib or their combination on cell cycle distribution. H1299 cells were treated with celecoxib or/and aspirin for 48 h. As shown in Figure 5(a), when H1299 cells were treated with 40 μ M celecoxib or 8 mM aspirin alone and compared with the control group, the number of cells in the G1 phase increased, whereas the number of cells in the G2 period decreased. Furthermore, the number of cells in the G1 phase of the combination group was the most pronounced, and the decrease in the number of cells in the G2 phase was also more obvious than it was in other phases. Therefore, celecoxib combined with aspirin changed the H1299 cell cycle and arrested the cells at the G1 phase.

We next examined the change in G1 phase-related proteins by western blot analysis. The results are shown in Figure 5(b). Compared with the control group, no significant change in cyclin-dependent kinase 2 (CDK2) protein expression

was observed in the cells treated with celecoxib or aspirin alone; however, when these two drugs were combined, the expression level of the CDK2 protein was markedly down-regulated ($p < 0.01$). In addition, the expression level of Cyclin D1 protein in celecoxib alone or in combination was significantly lower than it was in the control group ($p < 0.01$). P21 is a potent inhibitor of CDKs, and our data showed that the expression level of p21 protein was up-regulated in cells receiving a single treatment of aspirin or a combined treatment. Overall, our findings suggested that celecoxib combined with aspirin-initiated cell cycle arrest at the G0/G1 phase *via* the activation of p21 and subsequent inhibition of CDK2.

Identification of GRP78 as one of the target proteins of aspirin in A549 cells

To further investigate the molecular mechanism by which aspirin inhibits the growth of NSCLC cells, we referred to the related research of Wang *et al.*, who used chemical proteomics to identify the target proteins of aspirin in HCT116 cells.²¹ In summary, salicylic acid first reacted with acyl chloride to form Asp-P1 and Asp-P2 probes. Compared with aspirin, the probe has a tail with an ethynyl group, but showed similar physiological activity to aspirin and can simulate the acetylation of aspirin at the target protein. Next, the aspirin probe was co-incubated with HCT116 cells to achieve covalent labeling of aspirin target proteins through the reactive groups in the probe. After the labeling of the probe was completed, biotin was added to the probe as a reporter by using the biorthogonal reaction called “click chemistry”. Finally, the biotin-avidin method was used to enrich the biotin-labeled target protein with streptavidin beads. The proteins identified by the probe were thus the target proteins of aspirin, and 523 protein targets were confidently obtained after a series of experiments.²¹ Based on these target proteins, we used MetaCore™ software in the current study to analyze the experimental results previously obtained by Wang *et al.* As shown in Figure 6(a), the MetaCore™ pathway mapping tool clustered GRP78 in close association with aspirin with a high score, suggesting that GRP78, which is involved in endoplasmic reticulum stress, tumor growth and tumor drug resistance, might be a possible target protein of aspirin in cancer cells.

To verify whether GRP78 was the target protein of aspirin, the CDocker function in DS (DISCOVERY STUDIO) software was then used to simulate the binding of aspirin and

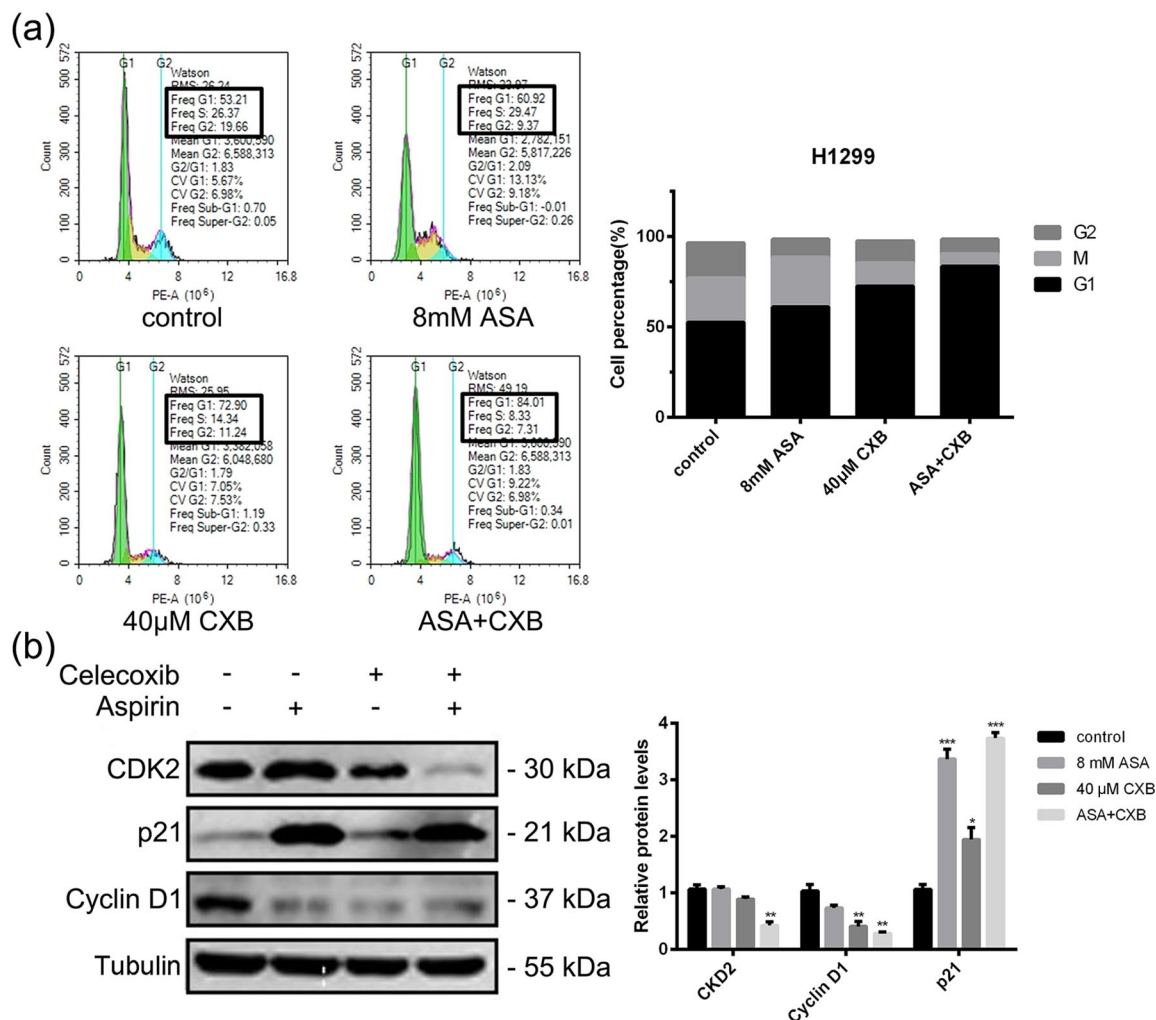


Figure 5. Effect of celecoxib and aspirin on cell cycle distribution. (a) H1299 cells were treated with celecoxib (40 µM) and/or aspirin (8 mM) for 48 h. The cells were then fixed with 70% ethanol and stained with propidium iodide. The cell cycle distribution (G0/G1, G2/M and S) was determined by flow cytometry analysis. (b) Western blotting was also performed to detect the levels of cell cycle regulators (Cyclin D1, CDK2 and p21). Band intensity was quantified by Image J software. The results shown are representative of three different experiments. Data are represented as mean ± SD.

**p* < 0.05

***p* < 0.01

****p* < 0.001

ASA, aspirin; CXB, celecoxib; PE-A, phycoerythrin area.

GRP78 protein. As shown in Figure 6(b), the two molecules successfully combined with the lowest conformational free energy. In addition, the binding site of aspirin is located at the adenosine triphosphate (ATP)-binding site of GRP78, which further supports the speculation that aspirin might inhibit GRP78 protein activity by competing with ATP for the binding site.

To further demonstrate that GRP78 protein is indeed the target protein of aspirin in cancer cells, we incubated the aspirin probes (Asp-P1 and

Asp-P2) with A549 cells for 12h and then extracted the proteins. After the biotin reporter group was added, the protein was enriched with streptavidin beads, and the target proteins obtained were then analyzed by western blot analysis to determine whether the GRP78 protein was among the target proteins bound to aspirin. As shown in Figure 6(c), the results indicated that, with the specific GRP78 antibody, no band representing the DMSO group control was apparent, but there was an obvious band corresponding to the Asp-P1 group. Interestingly, the band for the Asp-P2

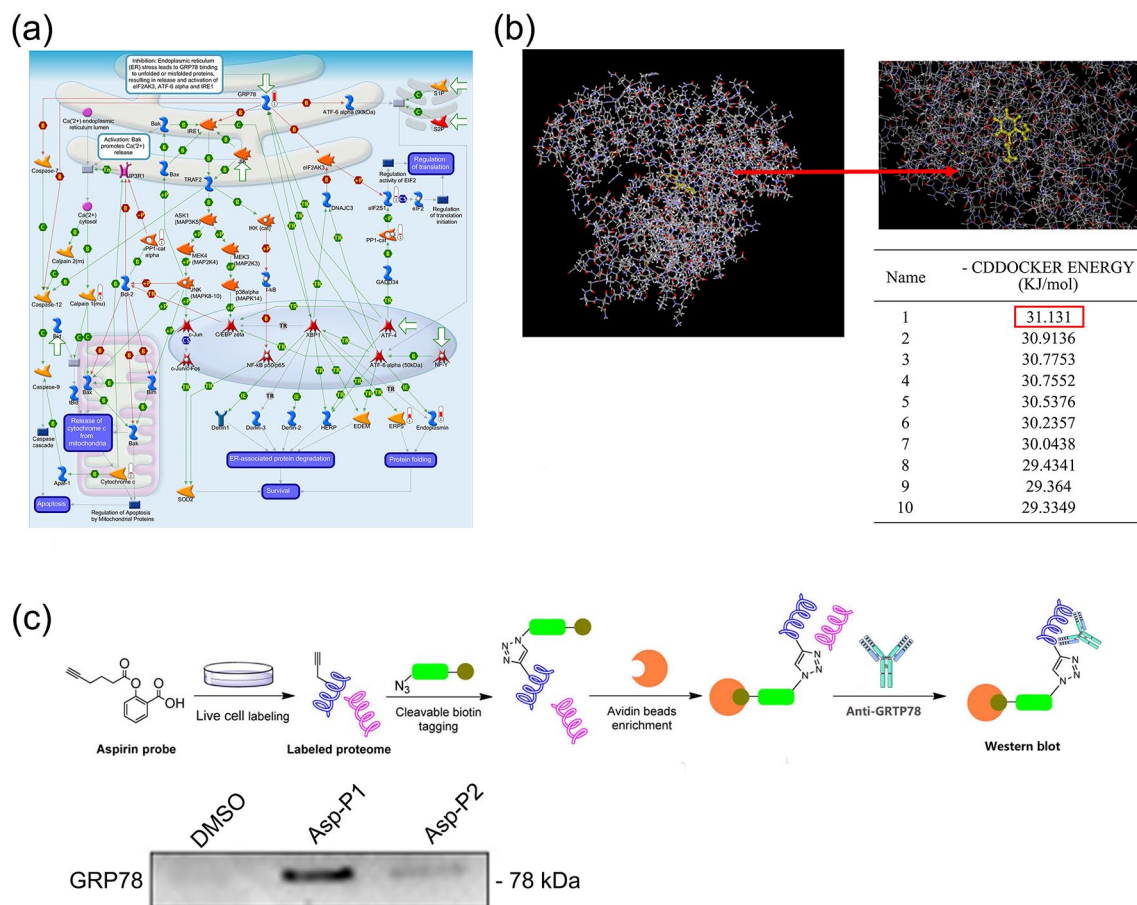


Figure 6. Identification of GRP78 as one of the target proteins of aspirin. (a) GeneGO pathway enrichment analysis of the target proteins of aspirin obtained by Jigang Wang *et al.*²¹ using MetaCore™ software. (b) The stereoscopic conformation of the binding of GRP78 protein to aspirin was analyzed by DS software, and the red arrow indicates the enlarged view at the binding site. The table shows 10 stereoscopic conformation of the GRP78 protein combined with aspirin, which was analyzed by DS software, and the first one was the lowest free energy conformation. (c) A549 cells were treated with 20 μ M aspirin probes (Asp-P1 and Asp-P2) and DMSO (negative control) for 12 h. The extracted protein was incubated with 10 μ M biotin-azide, 1 mM Tris[2-carboxyethyl]phosphine, 100 μ M Tris[[1-benzy-1H-1,2,3-triazol-4-yl)methyl]amine and 1 mM copper sulfate for 4 h. The proteins were precipitated, dried, redissolved and then incubated with streptavidin beads. After dissolving streptavidin beads, the supernatant was taken for western blotting for GRP78 detection. DMSO, dimethyl sulfoxide.

group was not obvious. The possible reason may be explained by the process of probe synthesis: the alkyne tail of the Asp-P1 probe is shorter than that of the Asp-P2 probe, making it easier for the former to compete for the ATP-binding site and to bind to the GRP78 protein at this site.

Aspirin and celecoxib in combination lead to endoplasmic reticulum (ER) stress-induced apoptosis by targeting GRP78

To examine the specific role of GRP78 in the aspirin-mediated anticancer effect, we next designed a GRP78-EGFP fusion protein with a

His-tag at the C-terminus. A Ni affinity chromatography column was used for the purification of this GRP78-EGFP protein. The target protein can be eluted by using an imidazole solution at a concentration of 50–100 mM. SDS-PAGE analysis revealed that the mobility of the purified protein corresponded to a molecular weight of approximately 72 kDa, which is consistent with the theoretical size of GRP78-EGFP, and no other bands appeared [Figure 7(a)]. Then, anti-GRP78 antibody was used to confirm the identity of the purified protein, and the result is shown in Figure 7(b). Next, we used MST to detect the binding of

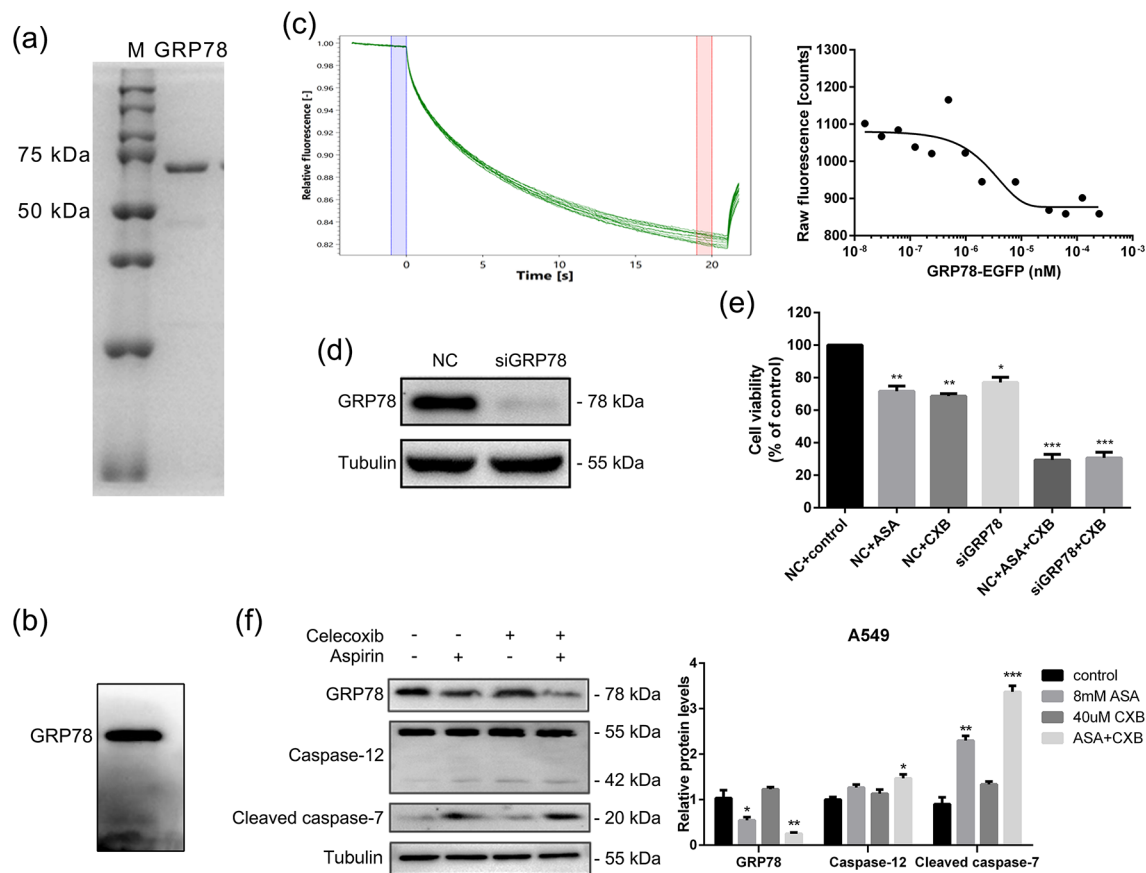


Figure 7. Aspirin and celecoxib in combination leads to ER stress-induced apoptosis by targeting GRP78. (a) His-tagged GRP78-EGFP was purified using a Ni affinity chromatography column. Gradient elution was performed using 50–100 mM imidazole solution. The elution of the target protein was identified using SDS-PAGE. (b) Western blotting analysis was used to confirm the purified protein with the anti-GRP78 antibody. (c) The microscale thermophoresis (MST) was used to detect the binding of gradient diluted aspirin to a fixed concentration of GRP78-EGFP *in vitro*. The results show fluorescence contrast before and after molecular thermophoresis and MST binding curves. (d) Effect of GRP78 interference fragment on its protein level by western blotting analysis. (e) A549 cells were transfected with GRP78 interference fragment or NC, and then treated with celecoxib (40 μ M) and/or aspirin (8 mM) for 48 h. The cell viability was assessed by CCK8 assay. (f) Effects of aspirin and celecoxib on the expression of caspase-7 and caspase-12 proteins. A549 cells were treated with aspirin (8 mM) and/or celecoxib (40 μ M). After 48 h, cells were harvested for western blotting analysis. The level of tubulin served as the loading control. Band intensities were calculated using software Image J. The results shown are representative of three different experiments. Data are represented as mean \pm SD.

* $p < 0.05$

** $p < 0.01$

*** $p < 0.001$

ASA, aspirin; CXB, celecoxib; ER, endoplasmic reticulum; NC, negative control.

GRP78-EGFP to aspirin at the molecular level *in vitro*. The concentration of GRP78-EGFP was fixed, and a gradient dilution was performed on non-fluorescent aspirin. MST surge is used to compare the fluorescence value F_{hot} (red) in a steady state after thermophoresis with the fluorescence value F_{cold} (blue) before the start of thermophoresis. The change in molecular thermophoresis is indicated by the normalized

fluorescence value ΔF_{norm} ($\Delta F_{\text{norm}} = F_{\text{hot}}/F_{\text{cold}}$). Since GRP78-EGFP binds to aspirin and changes its own thermophoresis, a unique detection curve is produced. Different concentrations of aspirin in different capillaries result in different thermophoretic detection signals. The fitted binding curve was plotted using ΔF_{norm} , and the value of the dissociation constant (K_d) was calculated as 1.6374 μ M, indicating that

GRP78-EGFP has a high binding affinity for aspirin [Figure 7(c)].

To further confirm the function of GRP78 in aspirin-mediated anticancer effects, we transfected A549 cells with NC and siGRP78 interference fragments. The interference efficiency of siGRP78 was verified by western blot analysis. As shown in Figure 7(d), the expression of GRP78 was significantly down-regulated in response to siGRP78 transfection. Next, celecoxib and aspirin were used alone or in combination to treat A549 cells transfected with NC and siGRP78 interference fragments for 48h, and cell viability was determined by CCK-8 assay. The results are shown in Figure 7(e). Single-transfection of the siGRP78 interference fragment inhibited the proliferation of A549 cells, and the cell viability decreased to 75% that of the control. Moreover, the inhibitory effect of aspirin and celecoxib on A549 cell viability was similar to that of siGRP78 and celecoxib in combination, further supporting the notion that aspirin might exert its anti-tumor effect mainly through the GRP78 protein. Thus, we speculated that one of the target proteins for the action of aspirin in A549 cells is likely to be GRP78.

Recently, it was reported that ectopically expressed GRP78 and caspase-7 and -12 could form a complex, thus coupling ER stress to the cell death program. In our present study, we observed the evident cleavage band of caspase-7 for the aspirin-treated group, and there was no significant cleavage band expression for the celecoxib-treated group. As shown in Figure 7(f), compared with that of either drug treatment alone, the cleavage band of caspase-7 was more obvious in the group of aspirin and celecoxib combined, indicating that aspirin and celecoxib in combination can induce caspase-7 activation. In addition, for the control group, caspase-12 did not show a cleavage band and the caspase-12 cleavage band was not obvious for either single-drug group; however, the cleavage of caspase-12 was apparent for the combination group. These results indicated that aspirin can target GRP78 and subsequently activate caspase-7 and caspase-12 when combined with celecoxib, thus leading to ER stress-induced apoptosis.

The combination of aspirin and celecoxib retards the development of lung cancer xenografts in nude mice

The anti-tumor effects of celecoxib and aspirin were measured in a xenograft tumor model by

transplanting A549 cells into athymic nude mice. Eight days post-implantation, the mice were randomly allocated into four groups with at least eight tumor-bearing mice per group. The tumor volume in the tumor-bearing mice was significantly reduced after 28 days of treatment with celecoxib and aspirin in combination compared with the volume in mice receiving either celecoxib or aspirin monotherapy. The use of celecoxib or aspirin alone inhibited the growth of xenograft tumors to some extent; however, the effect was not as significant as that of the combination therapy [Figure 8(a) and (b)]. At the end of the experiment, tumors from each mouse were removed and weighed. The combination treatment with celecoxib and aspirin significantly reduced tumor weight as compared with the control, celecoxib or aspirin groups [Figure 8(c)]. In addition, the combination of these two drugs significantly prolonged the TDT [Figure 8(d)], and the TGI value was also significantly enhanced, reaching nearly 60% efficiency [Figure 8(e)]. These data further showed that the combination of the two drugs had a good tumor suppressing effect. Moreover, there was no significant change in body weight of the mice in the four groups throughout the course of treatment [Figure 8(f)]. The liver and spleen of the mice in the monotherapy and combination treatment groups did not show significant swelling as compared with the control group (data not shown).

HE staining results further revealed that the tumor tissues of the mice treated with the combination of celecoxib and aspirin showed more severe necrosis than those of mice treated with celecoxib or aspirin monotherapy [Figure 8(g)]. TUNEL assay showed that a single treatment with celecoxib or aspirin had a promoting effect on the apoptosis rate of tumor tissues, but the apoptotic area affected by the combination therapy was significantly increased, indicating that the combination therapy inhibited tumor growth by inducing the apoptosis of cells *in vivo* [Figure 8(h)]. Immunohistochemistry analysis showed similar results. After combination therapy, the expression of cleaved caspase-3 in tumor tissues was significantly up-regulated compared with that in the celecoxib or aspirin monotherapy group, further confirming that the apoptosis rate of cells in the tumor tissues was significantly increased [Figure 8(i)].

Discussion

It is well known that cancer is a disease caused by the dysregulation of multiple signaling pathways.

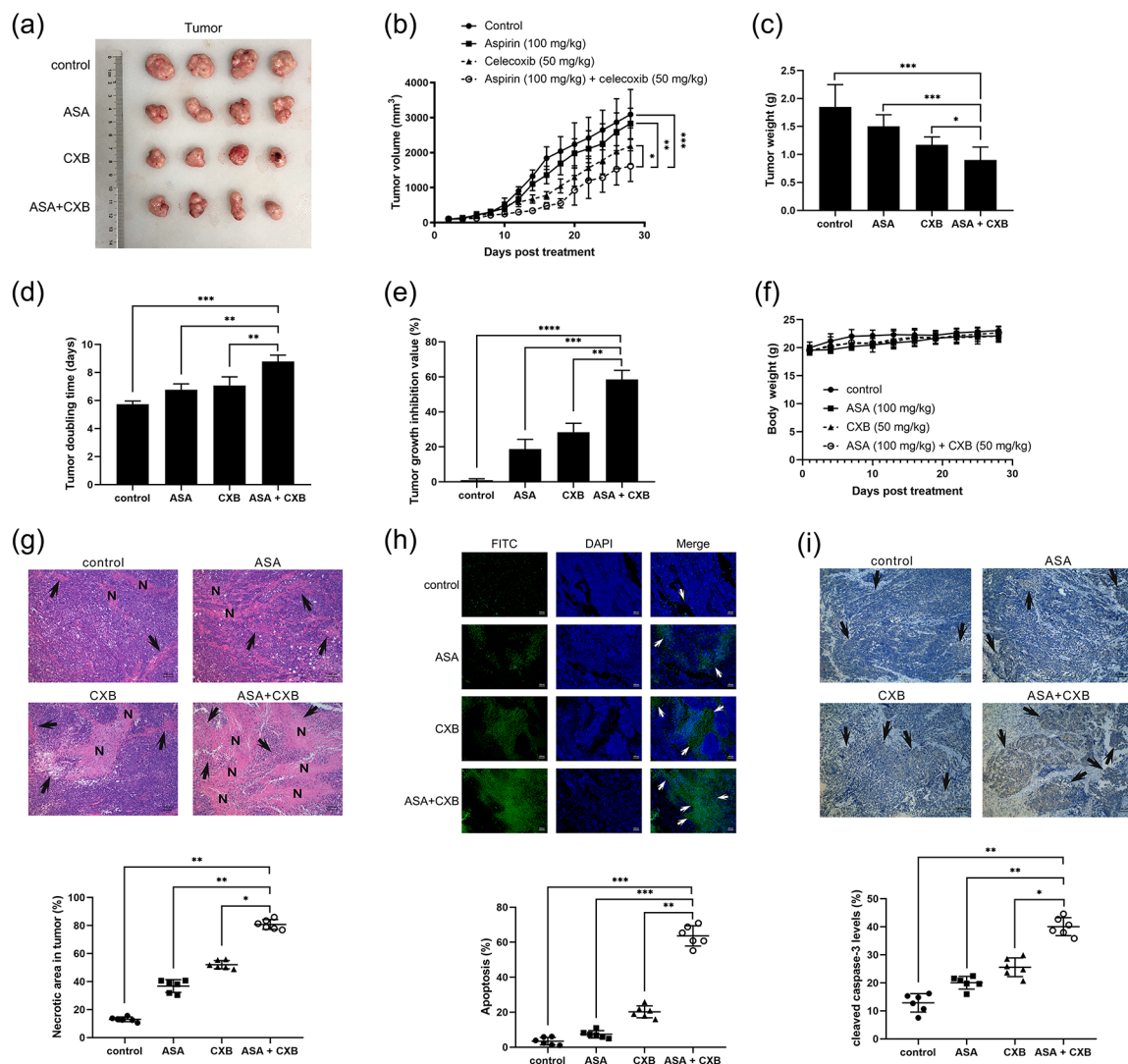


Figure 8. Celecoxib and aspirin combined therapy inhibits *in vivo* tumor xenograft growth in a subcutaneous tumor model. A549 cells were injected subcutaneously into the right axilla of athymic nude mice. When the tumor volume reached about 100–150 mm³, the mice were given an aqueous solution of aspirin daily or intraperitoneally with celecoxib or the combination of two drugs every other day for a total of 28 days. (a) Tumor photos of mice treated differently after 28 days of treatment. (b) Tumor volumes under different treatments were compared. (c) Tumor weight of mice treated differently after 28 days of treatment. (d) Tumor doubling time of each group. (e) Inhibition rate of different treatments on tumors in nude mice during treatment. (f) Body weight change during treatment. (g) Determination of tumor necrosis after combined treatment with celecoxib and aspirin. Tumor necrosis areas are shown by HE staining and observed under light microscope ($\times 100$). The viable tumor cells are indicated by a black arrow. Tumor necrosis was determined by software Image J. Two sections/mouse and four mice were prepared. (h) Determination of apoptosis after combined treatment with celecoxib and aspirin. TUNEL assay was used to detect apoptotic cells (stained green and indicated with white arrows) ($\times 100$). The ratio of apoptotic cells to total cells: TUNEL positive cells were counted from three fields of the highest density of positive-stained cells in each section to determine the percentage of apoptotic cells. (i) Immunohistochemistry was used to detect the expression of cleaved caspase-3 in tumor cells and observed using light microscope ($\times 100$). Black arrows are used to indicate areas where significant protein expression occurs. The area where the protein expression (brown spots) appeared was calculated as a percentage of the total area using Image J. Data are represented as mean \pm SD. **** $p < 0.0001$

ASA, aspirin; CXB, celecoxib; TUNEL, TdT-mediated dUTP nick end labeling; FITC, fluorescein isothiocyanate; DAPI, 2-(4-Aminophenyl)-6-indolecarbamidine dihydrochloride.

Treatment with a single drug usually has little effect. Combination therapy affecting multiple signaling pathways may be an improvement over monotherapy.³⁰ Therefore, we are currently exploring strategies for the combination of targeted drugs to treat cancer.³¹

It has been reported that COX-2 inhibitors promote the apoptosis of NSCLC cells and enhance the effect of chemotherapy. In addition, the use of COX-2 inhibitors can weaken the potential for immune escape by NSCLC cells, enhance the anti-tumor activity of PD-1/PD-L1-based immunotherapy and improve the efficacy of cancer treatment and the prognosis of patients.³² All of these findings provide a solid theoretical basis for using COX-2 inhibitors combined with other drugs to treat NSCLC. Celecoxib, a star-selective inhibitor of COX-2, has been reported to treat various types of cancer cells in humans and animals. Celecoxib has been reported to affect tumor cell apoptosis, proliferation, invasion and cell cycle through a mechanism that is dependent or independent of COX-2.⁸ To date, the apoptotic effect of celecoxib has been shown to be associated with multiple signaling pathways in the cell, such as those of mitogen-activated protein kinase (MAPK), NF- κ B and caspases.³³⁻³⁵ Current studies have shown that long-term and high-dose use of celecoxib, a drug in the COXIB family, causes cardiovascular toxicity and increases the risk of gastrointestinal diseases.³⁶⁻³⁹ Therefore, due to these concerns, when celecoxib is used as an anticancer drug, it is necessary to optimize the scheme, and we are considering the combination of celecoxib and other drugs to reduce the side effects of the drug itself and kill cancer cells at the same time.

A large number of studies show that aspirin has special potential in the prevention of cancer, especially colon cancer,⁴⁰⁻⁴⁴ and plays a specific role in cancer treatment.⁴⁵⁻⁴⁷ Therefore, the legend of aspirin for anti-tumor therapy was opened. However, there are relatively few reports of aspirin used against lung cancer, and the anticancer mechanism also remains unclear. In addition, in lung cancer, the combination of aspirin with other anti-cancer drugs has not been thoroughly explored.

Since both celecoxib and aspirin have anti-tumor activity, we speculate that the combination of these two drugs might be more effective than monotherapy in treating tumors. In this study, we aimed to investigate the effects of celecoxib and

aspirin alone or in combination on the proliferation, apoptosis, cell cycle and migration of NSCLC cells, and further explored the possible underlying mechanisms of action.

Using CCK-8, EdU, flow cytometry and TUNEL assays and other experimental methods, we found that celecoxib combined with aspirin inhibited cell proliferation and induced apoptosis to a significantly greater extent than that observed after treatment with either drug alone. It is well known that apoptosis is ultimately executed by caspase-3 through the modulation of multiple signaling pathways involved in apoptosis regulation. To further clarify the anticancer mechanism of celecoxib and aspirin treatment, we measured the expression levels of caspase-8, -9 and -3 to assess their activation levels. The results showed that celecoxib and aspirin in combination induced apoptosis of NSCLC cells by activating caspase-8, -9 and -3. Subsequently, activation of caspases leads to PARP cleavage and nuclear condensation, which ultimately results in apoptosis. Pro-apoptotic proteins (Bak, Bid and Bax) or anti-apoptotic proteins (Bcl-2 and Bcl-xl) in the Bcl-2 family proteins affect apoptosis by controlling the permeability of the mitochondrial outer membrane in the mitochondrial apoptosis pathway. Upregulation of the ratio of Bax:Bcl-2 results in the release of some pro-apoptotic proteins from mitochondria.⁴⁸ In our study, therapy of celecoxib combined with aspirin led to apparent down-regulation of Bcl-xl and Bcl-2 expression and upregulation of Bax expression, resulting in an increased proportion of Bax:Bcl-2. These results indicate that celecoxib combined with aspirin induced the apoptosis of A549 cells *via* a caspase-mediated mitochondrial pathway. Therefore, we conclude that aspirin can increase the sensitivity of A549 cells to celecoxib through the caspase-mediated apoptosis pathway and the endogenous apoptosis pathway.

ERK is an important component of MAPKs and plays an integral role in cell growth, proliferation, apoptosis and other activities. There is increasing evidence that changes in MAPK activity account for the role of anti-tumor drugs in a variety of cancer cell lines.⁴⁹ Therefore, treatment with drugs targeting the MAPK pathway is a promising NSCLC treatment strategy. In the current study, we provide evidence that celecoxib combined with aspirin inhibited ERK signaling, which was critical for inducing apoptosis in NSCLC cells.

Cell proliferation is the result of a transition of the cell cycle from a resting state to a progressing state. Flow cytometry results in our study showed that the combination of celecoxib and aspirin induced A549 cell cycle arrest in the G0/G1 phase. The progress of cell cycle is driven by the periodic activation and inactivation of the CDK-cyclin complex. Changes in the activity of these complexes affect the transition between phases, and this transition change is determined by the level of cyclins and the phosphorylation status of CDK.^{50,51} For example, in the early G1 phase, Cyclin D combines with CDK2 and CDK4 to form a complex that moves the cell cycle from the G1 to the G2 phase.⁵² P21 is a very important cyclin-dependent kinase inhibitor that can arrest cell cycle progression at the G1/S or G2/M transition by inhibiting CDK4/6-Cyclin D and CDK2-Cyclin E, respectively, and has the ability to inhibit cell cycle.⁵³ In addition, previous studies have shown that celecoxib can inhibit cell proliferation and carcinogenesis, reduce the activity of CDK proteins or induce the expression of p27 and p21, resulting in cell cycle arrest.^{54,55} In the current study, we observed that celecoxib and aspirin significantly up-regulated p21 protein expression levels, subsequently leading to negative regulation of the G1/S transition. Both Cyclin D1 and CDK2 are factors that can trigger the cell G1/S transition, and their reduction in response to the celecoxib and aspirin combined treatment may ultimately lead to cell cycle arrest.

There are many basic processes involved in the occurrence and development of cancer, including proliferation, invasion and metastasis, but all of them are closely related to the remodeling of extracellular matrix (ECM).⁵⁶ ECM is the basic barrier limiting cancer cell growth and proliferation. Tumor cells need to produce or induce proteases to degrade the ECM during the process of transferring through the natural barrier of tissue to the distant parts of the body. MMPs constitute a family of zinc-containing endopeptidases that play key roles in the degradation of ECM proteins.⁵⁷ Under normal physiological conditions, MMP is at a low level and is relatively less active because of the inhibition of tissue inhibitors of metalloproteinases.⁵⁷ However, in cancer tissues, the system for regulating the expression and activity of MMPs is dysfunctional. Many MMPs, including MMP-9, are overexpressed and overactivated, and this expression is up-regulated even more significantly in advanced cancer.⁵⁷⁻⁵⁹ In our study, we found that the combination of celecoxib

and aspirin inhibited the migration of NSCLC cells. Further exploration of its mechanism revealed that the expression of MMP-2 and MMP-9 proteins was significantly down-regulated when the two drugs were used in combination. Combining the results of previous experiments, we thus concluded that the combination of aspirin and celecoxib inhibits the ERK signaling pathway, possibly further inhibiting its binding to the MMP-2 and MMP-9 promoters, making the initiation of transcription and translation impossible; thus, MMP-2 and MMP-9 expression levels are down-regulated.

Currently, little research has been conducted on the targets of aspirin that confer the anti-tumor effect. In this study, based on the study by Wang *et al.*,²¹ we found that, among 523 protein targets that have been identified for aspirin, the GRP78 protein, which is associated with endoplasmic reticulum stress and tumor resistance, is likely to be one of the target proteins of aspirin in cancer cells. We next used molecular docking technology to demonstrate that the GRP78 protein is indeed a target protein for aspirin and that aspirin inhibits the activity of the GRP78 protein by competitively binding to the ATP-binding site, a finding consistent with previous speculation. We referred to the experimental scheme of Wang *et al.*²¹ and used aspirin probes (Asp-P1 and Asp-P2) in A549 cells to acetylate and label the target protein. Then, biotin-azide was introduced to connect biotin as a reporter group to the probe by a "CuAAC" reaction^{60,61} to mark the level of the target proteins in the proteome through the reaction group in the reactive molecular probe. Finally, streptavidin beads were used to enrich the proteins labeled by the probe through high affinity binding to biotin. After detection by a GRP78-specific antibody, we confirmed that the GRP78 protein in A549 cells was among the target proteins of aspirin. The MST assay further demonstrated a strong binding affinity for GRP78 protein with aspirin at the molecular level. After interfering with GRP78 in A549 cells, the inhibitory effect of celecoxib on A549 cells was similar to that of aspirin combined with celecoxib, indicating that aspirin might exert anti-tumor effects mainly through the GRP78 protein. The GRP78 protein is thus identified as the target protein for aspirin that exerts anti-tumor effects in A549 cells. Other study found that the expression of GRP78 was up-regulated in A549 cells treated with celecoxib.⁶² In our study, we also observed that the expression of GRP78 was slightly up-regulated when celecoxib was used alone to induce

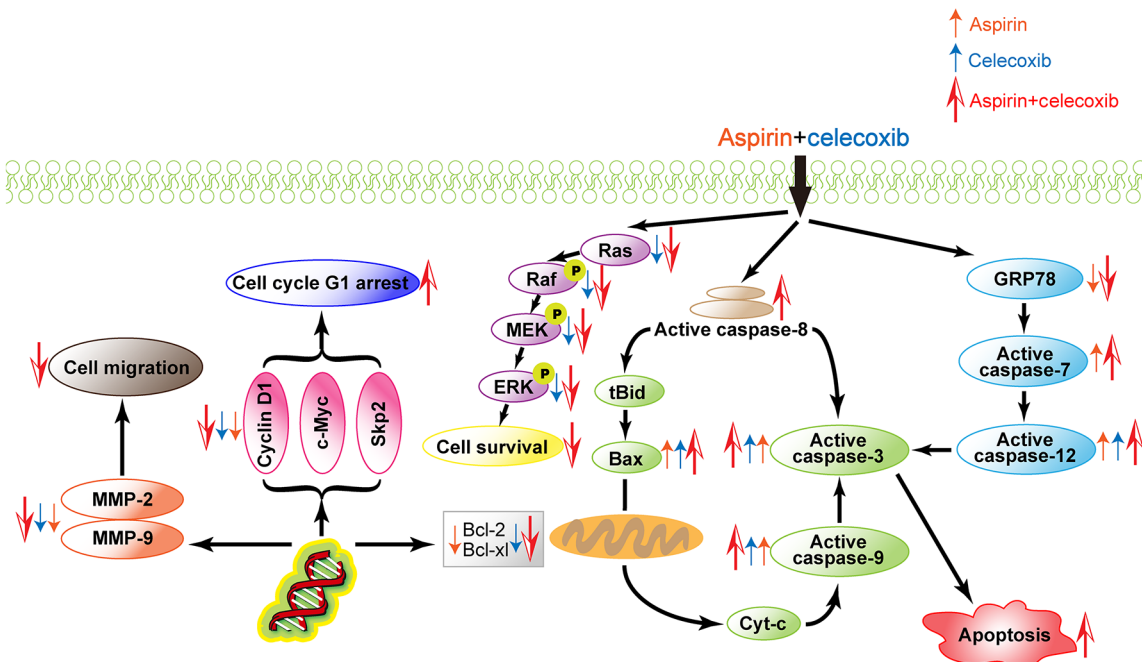


Figure 9. A working model for the synergistic effects of celecoxib and aspirin on non-small cell lung cancer (NSCLC) cells. In NSCLC cells, the combination of aspirin and celecoxib affects apoptosis through the mitochondrial apoptotic pathway. Down-regulation of Bcl-xl and Bcl-2, while up-regulating Bax, causes an increase in the ratio of Bax:Bcl-2 to induce the depolarization of the mitochondrial membrane with the release of cytochrome c and the consequent activation of caspase-9 and caspase-3, resulting in apoptosis of NSCLC cells. Abnormal expression of cell cycle regulators, such as Cyclin D1, CDK2 and p21, leads to cell cycle G1 arrest and ultimately promotes apoptosis. At the same time, the expression of MMP-2 and MMP-9 proteins was significantly down-regulated, which inhibited the migration and invasion of tumor cells. The ERK signaling pathway was also significantly inhibited in response to aspirin and celecoxib in combination and cell survival thus decreased. In addition, aspirin activates caspase-7 and caspase-12 *via* inhibiting the expression of GRP78 protein, further enhancing ER stress-induced apoptosis. All of the previous may account for the synergistic effects of celecoxib and aspirin on NSCLC cells. ERK, extracellular signal-regulated kinase; ER, endoplasmic reticulum.

apoptosis. However, when celecoxib and aspirin were combined, the expression of GRP78 was significantly down-regulated. Therefore, we speculate that aspirin might inhibit the expression of GRP78 by targeting GRP78 and thus promote apoptosis of A549 cells, a finding consistent with the results obtained by Kim *et al.*,⁶² in which siGRP78 was used to decrease the expression of GRP78 and sensitized A549 cells to celecoxib-induced apoptosis. This outcome indicates that when celecoxib induces apoptosis of cells in NSCLC, aspirin may reduce tumor resistance by inhibiting the expression of GRP78, which would further activate the endoplasmic reticulum stress response, the downstream caspase signaling pathway and the activity of pro-apoptotic proteins in the Bcl-2 protein family. In general, the combination of aspirin and celecoxib causes sustained endoplasmic reticulum stress, which can ultimately induce apoptosis through the non-mitochondrial pathway and the

mitochondrial pathway, and GRP78 might be a key target protein in this process.

To extend the observations made in cultured cells, we determined the effect of combined treatment with celecoxib and aspirin on the growth of lung cancer xenografts in nude mice. Our results show that the combined treatment had a significant effect on the inhibition of tumor growth in the xenograft model. The use of aspirin or celecoxib alone inhibited tumor growth to a certain extent, but the effect was not as good as the combination treatment. In addition, no general signs of toxicity were observed in any groups. After HE staining, we found that the combination treatment increased tumor tissue necrosis. TUNEL staining and immunohistochemistry further demonstrated that celecoxib combined with aspirin increased the apoptosis of tumor tissue cells *in vivo*, which indicated that the inhibition of

tumor growth by the combined use of celecoxib and aspirin might be caused by apoptotic cell death. However, in addition to inducing apoptosis, there are probably additional mechanisms through which combination therapy can inhibit tumor growth; however, these mechanisms remain to be elucidated in the future.

Conclusion

In conclusion, this study provides compelling evidence that the combination of celecoxib and aspirin significantly leads to suppression of NSCLC cell proliferation, migration and invasion, arrest in cell cycle, and induction of apoptosis, and that these effects are more pronounced than they are after treatment with either drug alone. Further investigation of the mechanism of action of these drugs revealed that the combination of celecoxib and aspirin mainly exerts anti-tumor effects by activating the signaling pathways involved in caspase activation and cell cycle arrest in G1, and inhibiting the ERK–MAPK signaling pathway and the activity of MMP-9. In addition, GRP78 might be one of the important targets of aspirin in NSCLC cells, and the combination of aspirin and celecoxib may thus cause sustained endoplasmic reticulum stress, ultimately leading to the induction of apoptosis (Figure 9). Therefore, it is worthwhile to consider this combination treatment for use in NSCLC and it warrants further evaluation in clinical trials.

Author contributions

HZ, ZCH and JW designed the outline of the paper. HZ revised this manuscript. XZ, JC and CC contributed equally to this work. XZ and JC performed most of the experiments in this study. XZ and JC wrote the manuscript and prepared the figures. CC performed GRP78 expression and purification experiments. PL, YL, HX, JL and NC helped with the cell related experiments. FC helped with the experiments using animals. All authors have read and approved the final version of this manuscript.

Conflict of interest statement

The authors declare that there is no conflict of interest.

Ethics statement

Animal welfare and experimental procedures were performed in strict accordance with high standard animal welfare and other related ethical regulations approved by Nanjing University.

Funding

The authors disclosed receipt of the following financial support for the research, authorship, and/or publication of this article: this study was supported by grants from the Chinese National Natural Sciences Foundation (81773099 and 81630092) and the National Key R&D Program of China (2017YFA0506000).

Supplemental material

Supplemental material for this article is available online.

References

1. Bray F, Ferlay J, Soerjomataram I, *et al.* Global cancer statistics 2018: GLOBOCAN estimates of incidence and mortality worldwide for 36 cancers in 185 countries. *CA Cancer J Clin* 2018; 68: 394–424.
2. Pirker R. Conquering lung cancer: current status and prospects for the future. *Pulmonology*. Epub ahead of print 18 March 2020. DOI: 10.1016/j.pulmoe.2020.02.005.
3. Rotow J and Bivona TG. Understanding and targeting resistance mechanisms in NSCLC. *Nat Rev Cancer* 2017; 17: 637–658.
4. Song Y, Zhong X, Gao P, *et al.* Aspirin and its potential preventive role in cancer: an umbrella review. *Front Endocrinol (Lausanne)* 2020; 11: 3.
5. Ye S, Lee M, Lee D, *et al.* Association of long-term use of low-dose aspirin as chemoprevention with risk of lung cancer. *JAMA Netw Open* 2019; 2: e190185.
6. Marsico F, Paolillo S and Filardi PP. NSAIDs and cardiovascular risk. *J Cardiovasc Med (Hagerstown)* 2017; 18(Suppl. 1): Special issue on the state of the art for the practicing cardiologist: the 2016 Conoscere E Curare Il Cuore (CCC) Proceedings from the CLI Foundation: e40–e43.
7. Yi C, Wang Y, Zhang C, *et al.* Cleavage and polyadenylation specific factor 4 targets NF- κ B/cyclooxygenase-2 signaling to promote lung cancer growth and progression. *Cancer Lett* 2016; 381: 1–13.
8. Bourn J, Pandey S, Uddin J, *et al.* Detection of tyrosine kinase inhibitors-induced COX-2 expression in bladder cancer by fluorocoxib A. *Oncotarget* 2019; 10: 5168–5180.
9. Fu X, Zhang H, Chen Z, *et al.* TFAP2B overexpression contributes to tumor growth and progression of thyroid cancer through the COX-2 signaling pathway. *Cell Death Dis* 2019; 10: 397.

10. Jendrossek V, Handrick R and Belka C. Celecoxib activates a novel mitochondrial apoptosis signaling pathway. *FASEB J* 2003; 17: 1547–1549.
11. Leahy KM, Ornberg RL, Wang Y, *et al.* Cyclooxygenase-2 inhibition by celecoxib reduces proliferation and induces apoptosis in angiogenic endothelial cells in vivo. *Cancer Res* 2002; 62: 625–631.
12. Gulyas M, Mattsson JSM, Lindgren A, *et al.* COX-2 expression and effects of celecoxib in addition to standard chemotherapy in advanced non-small cell lung cancer. *Acta Oncol* 2018; 57: 244–250.
13. Elmets CA, Viner JL, Pentland AP, *et al.* Chemoprevention of nonmelanoma skin cancer with celecoxib: a randomized, double-blind, placebo-controlled trial. *J Natl Cancer Inst* 2010; 102: 1835–1844.
14. Bastos-Pereira AL, Lugarini D, Oliveira-Christoff A, *et al.* Celecoxib prevents tumor growth in an animal model by a COX-2 independent mechanism. *Cancer Chemother Pharmacol* 2010; 65: 267–276.
15. Ralph SJ, Nozuhur S, Moreno-Sánchez R, *et al.* NSAID celecoxib: a potent mitochondrial pro-oxidant cytotoxic agent sensitizing metastatic cancers and cancer stem cells to chemotherapy. *J Cancer Metastasis Treat* 2018; 4: 49.
16. Jeon YW and Suh YJ. Synergistic apoptotic effect of celecoxib and luteolin on breast cancer cells. *Oncol Rep* 2013; 29: 819–825.
17. Canney PA, Machin MA and Curto J. A feasibility study of the efficacy and tolerability of the combination of exemestane with the COX-2 inhibitor celecoxib in post-menopausal patients with advanced breast cancer. *Eur J Cancer* 2006; 42: 2751–2756.
18. Rotte A. Combination of CTLA-4 and PD-1 blockers for treatment of cancer. *J Exp Clin Cancer Res* 2019; 38: 255.
19. Hemati M, Haghirsadat F, Yazdian F, *et al.* Development and characterization of a novel cationic PEGylated niosome-encapsulated forms of doxorubicin, quercetin and siRNA for the treatment of cancer by using combination therapy. *Artif Cells Nanomed Biotechnol* 2019; 47: 1295–1311.
20. Wan X, Min Y, Bludau H, *et al.* Drug combination synergy in worm-like polymeric micelles improves treatment outcome for small cell and non-small cell lung cancer. *ACS Nano* 2018; 12: 2426–2439.
21. Wang J, Zhang CJ, Zhang J, *et al.* Mapping sites of aspirin-induced acetylations in live cells by quantitative acid-cleavable activity-based protein profiling (QA-ABPP). *Sci Rep* 2015; 5: 7896.
22. Tanhaian A, Mohammadi E, Vakili-Ghartavol R, *et al.* In silico and in vitro investigation of a likely pathway for anti-cancerous effect of Thrombocidin-1 as a novel anticancer peptide. *Protein Pept Lett.* Epub ahead of print 18 February 2020. DOI: 10.2174/0929866527666200219115129.
23. Spriestersbach A, Kubicek J, Schäfer F, *et al.* Purification of his-tagged proteins. *Methods Enzymol* 2015; 559: 1–15.
24. Dang LH, Bettgowda C, Huso DL, *et al.* Combination bacteriolytic therapy for the treatment of experimental tumors. *Proc Natl Acad Sci U S A* 2001; 98: 15155–15160.
25. Schwartz M. A biomathematical approach to clinical tumor growth. *Cancer* 1961; 14: 1272–1294.
26. Iqbal U, Yang HC, Jian WS, *et al.* Does aspirin use reduce the risk for cancer? *J Investig Med* 2017; 65: 391–392.
27. Pritchard R, Rodríguez-Enríquez S, Pacheco-Velázquez SC, *et al.* Celecoxib inhibits mitochondrial O₂ consumption, promoting ROS dependent death of murine and human metastatic cancer cells via the apoptotic signalling pathway. *Biochem Pharmacol* 2018; 154: 318–334.
28. Rohani MG and Parks WC. Matrix remodeling by MMPs during wound repair. *Matrix Biol* 2015; 44–46: 113–121.
29. Tai Y, Zhang LH, Gao JH, *et al.* Suppressing growth and invasion of human hepatocellular carcinoma cells by celecoxib through inhibition of cyclooxygenase-2. *Cancer Manag Res* 2019; 11: 2831–2848.
30. Mokhtari RB, Homayouni TS, Baluch N, *et al.* Combination therapy in combating cancer. *Oncotarget* 2017; 8: 38022–38043.
31. Lopez JS and Banerji U. Combine and conquer: challenges for targeted therapy combinations in early phase trials. *Nat Rev Clin Oncol* 2017; 14: 57–66.
32. Nichetti F, Ligorio F, Zattarin E, *et al.* Is there an interplay between immune checkpoint inhibitors, thromboprophylactic treatments and thromboembolic events? Mechanisms and impact in non-small cell lung cancer patients. *Cancers (Basel)* 2019; 12: 67.
33. Wang G, Li J, Zhang L, *et al.* Celecoxib induced apoptosis against different breast cancer cell lines

- by down-regulated NF- κ B pathway. *Biochem Biophys Res Commun* 2017; 490: 969–976.
34. Hassanzade A, Mandegary A, Sharif E, *et al.* Cyclooxygenase inhibitors combined with deuterium-enriched water augment cytotoxicity in A549 lung cancer cell line via activation of apoptosis and MAPK pathways. *Iran J Basic Med Sci* 2018; 21: 508–516.
 35. Abdelrahman RS and Abdelmageed ME. Renoprotective effect of celecoxib against gentamicin-induced nephrotoxicity through suppressing NF κ B and caspase-3 signaling pathways in rats. *Chem Biol Interact* 2020; 315: 108863.
 36. Jendrossek V. Targeting apoptosis pathways by celecoxib in cancer. *Cancer Lett* 2013; 332: 313–324.
 37. McGettigan P and Henry D. Cardiovascular risk and inhibition of cyclooxygenase: a systematic review of the observational studies of selective and nonselective inhibitors of cyclooxygenase 2. *JAMA* 2006; 296: 1633–1644.
 38. Schönthal AH, Chen TC, Hofman FM, *et al.* Celecoxib analogs that lack COX-2 inhibitory function: preclinical development of novel anticancer drugs. *Expert Opin Investig Drugs* 2008; 17: 197–208.
 39. Sooriakumaran P, Langley SE, Laing RW, *et al.* COX-2 inhibition: a possible role in the management of prostate cancer? *J Chemother* 2007; 19: 21–32.
 40. Drew DA, Cao Y and Chan AT. Aspirin and colorectal cancer: the promise of precision chemoprevention. *Nat Rev Cancer* 2016; 16: 173–186.
 41. Patrignani P and Patrono C. Aspirin and cancer. *J Am Coll Cardiol* 2016; 68: 967–976.
 42. Sivarasan N and Smith G. Role of aspirin in chemoprevention of esophageal adenocarcinoma: a meta-analysis. *J Dig Dis* 2013; 14: 222–230.
 43. Ye X, Fu J, Yang Y, *et al.* Frequency-risk and duration-risk relationships between aspirin use and gastric cancer: a systematic review and meta-analysis. *PLoS One* 2013; 8: e71522.
 44. Vidal AC, Howard LE, Moreira DM, *et al.* Aspirin, NSAIDs, and risk of prostate cancer: results from the REDUCE study. *Clin Cancer Res* 2015; 21: 756–762.
 45. Gu M, Nishihara R, Chen Y, *et al.* Aspirin exerts high anti-cancer activity in PIK3CA-mutant colon cancer cells. *Oncotarget* 2017; 8: 87379–87389.
 46. Henry WS, Laszewski T, Tsang T, *et al.* Aspirin suppresses growth in PI3K-mutant breast cancer by activating AMPK and inhibiting mTORC1 signaling. *Cancer Res* 2017; 77: 790–801.
 47. Jiang MJ, Dai JJ, Gu DN, *et al.* Aspirin in pancreatic cancer: chemopreventive effects and therapeutic potentials. *Biochim Biophys Acta* 2016; 1866: 163–176.
 48. Yang Y, Zong M, Xu W, *et al.* Natural pyrethrins induces apoptosis in human hepatocyte cells via Bax- and Bcl-2-mediated mitochondrial pathway. *Chem Biol Interact* 2017; 262: 38–45.
 49. Chong H, Vikis HG and Guan KL. Mechanisms of regulating the Raf kinase family. *Cell Signal* 2003; 15: 463–469.
 50. Nurse P. Universal control mechanism regulating onset of M-phase. *Nature* 1990; 344: 503–508.
 51. Dash BC and El-Deiry WS. Cell cycle checkpoint control mechanisms that can be disrupted in cancer. *Methods Mol Biol* 2004; 280: 99–161.
 52. Neganova I and Lako M. G1 to S phase cell cycle transition in somatic and embryonic stem cells. *J Anat* 2008; 213: 30–44.
 53. Karimian A, Ahmadi Y and Yousefi B. Multiple functions of p21 in cell cycle, apoptosis and transcriptional regulation after DNA damage. *DNA Repair (Amst)* 2016; 42: 63–71.
 54. Schönthal AH. Direct non-cyclooxygenase-2 targets of celecoxib and their potential relevance for cancer therapy. *Br J Cancer* 2007; 97: 1465–1468.
 55. Li G, Wang X, Luo Q, *et al.* Identification of key genes and long non-coding RNAs in celecoxib-treated lung squamous cell carcinoma cell line by RNA-sequencing. *Mol Med Rep* 2018; 17: 6456–6464.
 56. Kessenbrock K, Plaks V and Werb Z. Matrix metalloproteinases: regulators of the tumor microenvironment. *Cell* 2010; 141: 52–67.
 57. Nagase H, Visse R and Murphy G. Structure and function of matrix metalloproteinases and TIMPs. *Cardiovasc Res* 2006; 69: 562–573.
 58. Egeblad M and Werb Z. New functions for the matrix metalloproteinases in cancer progression. *Nat Rev Cancer* 2002; 2: 161–174.
 59. Yao Q, Kou L, Tu Y, *et al.* MMP-responsive ‘Smart’ drug delivery and tumor targeting. *Trends Pharmacol Sci* 2018; 39: 766–781.

60. Rostovtsev VV, Green LG, Fokin VV, *et al.*
A stepwise Huisgen cycloaddition process:
copper(I)-catalyzed regioselective “ligation” of
azides and terminal alkynes. *Angew Chem Int Ed
Engl* 2002; 41: 2596–2599.
61. Speers AE, Adam GC and Cravatt BF.
Activity-based protein profiling in vivo using
a copper(i)-catalyzed azide-alkyne [3 + 2]
cycloaddition. *J Am Chem Soc* 2003; 125:
4686–4687.
62. Kim B, Kim J and Kim YS. Celecoxib induces
cell death on non-small cell lung cancer cells
through endoplasmic reticulum stress. *Anat Cell
Biol* 2017; 50: 293–300.

Visit SAGE journals online
[journals.sagepub.com/
home/tam](http://journals.sagepub.com/home/tam)

 SAGE journals